

University of Massachusetts Amherst

From the Selected Works of Patrick Flaherty

Summer June 23, 2015

Identification of a new class of antifungals targeting the synthesis of fungal sphingolipids

Patrick Flaherty



Available at: <https://works.bepress.com/patrick-flaherty/13/>

Identification of a New Class of Antifungals Targeting the Synthesis of Fungal Sphingolipids

Visesato Mor, Antonella Rella, Amir M. Farnoud, Ashutosh Singh, Mansa Munshi, Arielle Bryan, Shamooun Naseem, James B. Konopka, Iwao Ojima, Erika Bullesbach, Alan Ashbaugh, Michael J. Linke, Melanie Cushion, Margaret Collins, Hari Krishna Ananthula, Larry Sallans, Pankaj B. Desai, Nathan P. Wiederhold, Annette W. Fothergill, William R. Kirkpatrick, Thomas Patterson, Lai Hong Wong, Sunita Sinha, Guri Giaever, Corey Nislow, Patrick Flaherty, Xuewen Pan, Gabriele Vargas Cesar, Patricia de Melo Tavares, Susana Frases, Kildare Miranda, Marcio L. Rodrigues, Chiara Luberto, Leonardo Nimrichter, Maurizio Del Poeta

ABSTRACT Recent estimates suggest that >300 million people are afflicted by serious fungal infections worldwide. Current antifungal drugs are static and toxic and/or have a narrow spectrum of activity. Thus, there is an urgent need for the development of new antifungal drugs. The fungal sphingolipid glucosylceramide (GlcCer) is critical in promoting virulence of a variety of human-pathogenic fungi. In this study, we screened a synthetic drug library for compounds that target the synthesis of fungal, but not mammalian, GlcCer and found two compounds [*N'*-(3-bromo-4-hydroxybenzylidene)-2-methylbenzohydrazide (BHBM) and its derivative, 3-bromo-*N'*-(3-bromo-4-hydroxybenzylidene) benzohydrazide (D0)] that were highly effective *in vitro* and *in vivo* against several pathogenic fungi. BHBM and D0 were well tolerated in animals and are highly synergistic or additive to current antifungals. BHBM and D0 significantly affected fungal cell morphology and resulted in the accumulation of intracellular vesicles. Deep-sequencing analysis of drug-resistant mutants revealed that four protein products, encoded by genes *APL5*, *COS111*, *MKK1*, and *STE2*, which are involved in vesicular transport and cell cycle progression, are targeted by BHBM.

IMPORTANCE Fungal infections are a significant cause of morbidity and mortality worldwide. Current antifungal drugs suffer from various drawbacks, including toxicity, drug resistance, and narrow spectrum of activity. In this study, we have demonstrated that pharmaceutical inhibition of fungal glucosylceramide presents a new opportunity to treat cryptococcosis and various other fungal infections. In addition to being effective against pathogenic fungi, the compounds discovered in this study were well tolerated by animals and additive to current antifungals. These findings suggest that these drugs might pave the way for the development of a new class of antifungals.

Recent estimates suggest that >300 million people are afflicted by serious fungal infections worldwide, with the most common and life-threatening invasive mycoses being cryptococcosis, candidiasis, aspergillosis, and pneumocystosis (1, 2). The number of fungal infections is rising in part due to the increasing number of individuals with immunocompro-

mising medical conditions such as AIDS or those using immunosuppressive medical treatment, such as some cancer therapies (3). Three classes of antifungal drugs are currently available: azoles (e.g., fluconazole), polyenes (e.g., amphotericin B), and echinocandins (e.g., caspofungin). However, these drugs are static and toxic, have a narrow spectrum of activity,

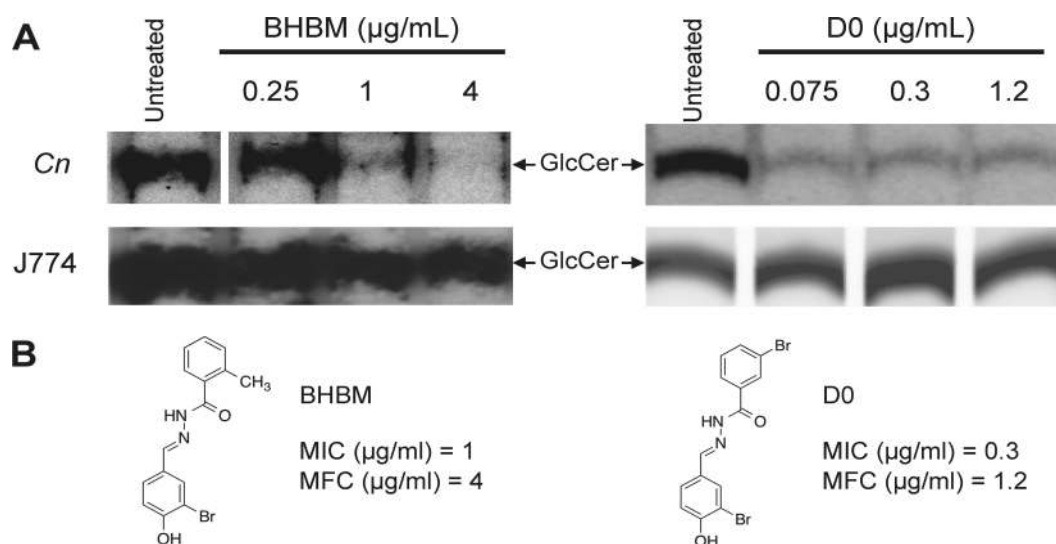


FIG 1 BHBM and D0 inhibit the synthesis of fungal but not mammalian glucosylceramide. (A) Thin-layer chromatography analysis of the synthesis of glucosylceramide (GlcCer) upon *in vivo* labeling of *C. neoformans* (*Cn*) or J774 cells with [^3H]palmitate and treated with BHBM or D0 at the indicated concentrations. (B) Structure of *N'*-(3-bromo-4-hydroxybenzylidene)-2-methylbenzohydrazide (BHBM) and 3-bromo-*N'*-(3-bromo-4-hydroxybenzylidene) benzohydrazide (D0). The MIC and minimum fungicidal concentration (MFC) are shown. Representative data of three independent experiments are shown.

and interact with other drugs such as chemotherapy agents and immunosuppressants (4).

Due to the limited number of antifungals available on the market, their increasing use stimulates the development of drug resistance, and thus, new classes of antifungals are desperately needed. The fungal sphingolipid glucosylceramide (GlcCer) is critical in promoting virulence of several plant- and human-pathogenic fungi, including *Cryptococcus neoformans*, *Candida albicans*, and *Aspergillus fumigatus* (5–10).

GlcCer regulates fungal cell replication in environments of neutral or alkaline pH (5, 11). When fungal cells lacking GlcCer are exposed to neutral/alkaline pH, they cannot progress through the cell cycle, and cytokinesis does not occur (5, 9, 12). GlcCer is most likely a panfungal virulence factor required during infection to promote fungal growth at neutral/alkaline environments in the host (e.g., alveolar spaces, cerebrospinal fluid, and bloodstream); as such, it is a promising novel drug target.

Antibodies to fungal GlcCer exert antifungal effects *in vitro* and *in vivo* (13); however, inhibitors that block fungal, but not mammalian, GlcCer synthesis are not available. In this study, we screened a synthetic drug library for compounds that specifically target the synthesis of fungal GlcCer. Two such compounds were found [*N'*-(3-bromo-4-hydroxybenzylidene)-2-methylbenzohydrazide (BHBM) and 3-bromo-*N'*-(3-bromo-4-hydroxybenzylidene) benzohydrazide (D0)] and were highly effective *in vitro* and *in vivo* against a series of pathogenic fungi. These compounds are safe and well tolerated in animals, demonstrate good pharmacokinetic properties, and are highly synergistic or additive to current antifungals. The compounds target the transport of fungal vesicles, which is how fungal ceramide is transported for the synthesis of GlcCer. Thus, we have identified a new class of antifungals that could potentially be used alone or in combination with existing antifungal drugs.

RESULTS

BHBM and D0 inhibit the synthesis of GlcCer. GlcCer regulates the growth of *C. neoformans* in neutral and alkaline pH (14). This

phenotype was utilized for screening of compounds that can inhibit fungal GlcCer. A ChemBridge DIVERSet-CL library containing 49,120 compounds was screened to identify molecules that inhibit the growth of *C. neoformans* at neutral and alkaline pH. A total of 220 compounds with a MIC of ≤ 1 $\mu\text{g/ml}$ were selected and screened in acidic (4.0) pH. The 18 compounds that were inactive (MIC > 32 $\mu\text{g/ml}$) were subjected to an *in vivo* labeling assay for the inhibition of GlcCer synthesis. Two compounds, identified as *N'*-(3-bromo-4-hydroxybenzylidene)-2-methylbenzohydrazide (BHBM) and 3-bromo-*N'*-(3-bromo-4-hydroxybenzylidene) benzohydrazide (D0), a derivative of BHBM, significantly inhibited the synthesis of GlcCer in *C. neoformans* but not mammalian (J774.16) cells (Fig. 1). Both compounds were fungicidal *in vitro* with minimum fungicidal concentrations (MFC) of 4 $\mu\text{g/ml}$ for BHBM and 1.2 $\mu\text{g/ml}$ for D0. Because of their structure, we designated this class of compounds “hydrazycins.”

BHBM and D0 exert antifungal activity. The antifungal activity of BHBM was examined against a variety of clinically relevant fungi (Table 1). BHBM showed good *in vitro* activity against various *Cryptococcus* species with the MIC ranging between 0.25 $\mu\text{g/ml}$ and 8 $\mu\text{g/ml}$. Importantly, a fluconazole-resistant *C. neoformans* strain (MIC > 64 $\mu\text{g/ml}$) and various virulent *Cryptococcus gattii* strains were highly susceptible to BHBM (MICs of 1 to 2 $\mu\text{g/ml}$ and 0.5 to 2 $\mu\text{g/ml}$, respectively). Other fungi against which BHBM was highly active included *Rhizopus oryzae*, *Blastomyces dermatitis*, *Histoplasma capsulatum*, *Pneumocystis murina*, and *Pneumocystis jirovecii* (Table 2). BHBM showed moderate activity (MIC range of 2 to 32 $\mu\text{g/ml}$) against *Candida krusei*, *Candida glabrata* (depending on the strain), *Candida guilliermondii*, *Candida parapsilosis*, *A. fumigatus*, and *Coccidioides* spp. and poor activity (MIC > 32 $\mu\text{g/ml}$) against *C. albicans*, *Candida parapsilosis*, and *Paecilomyces variotii* (Table 1). In addition, both BHBM and D0 were highly synergistic when combined with fluconazole and amphotericin B and additive when combined with caspofungin (see Table S1 in the supplemental mate-

TABLE 1 *In vitro* antifungal activities of *N'*-(3-bromo-4-hydroxybenzylidene)-2-methylbenzohydrazide (BHBM) determined by the MICs against several fungal clinical isolates and reference strains

Species (strain ^a) (n)	MIC range ($\mu\text{g/ml}$)
<i>Cryptococcus neoformans</i> (FTL strains) (13)	0.25–8
<i>Cryptococcus neoformans</i> (MDPL strains and S isolates) (8)	0.5–2
<i>Cryptococcus neoformans</i> (MDPL strains and R isolates) (4)	1–2
<i>Cryptococcus gattii</i> (FTL strains) (10)	0.5–2
<i>Cryptococcus gattii</i> (MDPL strains) (3)	0.5–1
<i>Candida albicans</i> (FTL strains) (3)	> 32
<i>Candida albicans</i> (MDPL strains) (5)	> 32
<i>Candida krusei</i> (MDPL strain) (1)	32
<i>Candida krusei</i> ATCC 6258 (MDPL strain)	16
<i>Candida krusei</i> QC FTL strains	8
<i>Candida glabrata</i> (FTL strains) (10)	0.125–2
<i>Candida glabrata</i> (MDPL strains) (3)	4– > 32
<i>Candida parapsilosis</i> (MDPL strains) (3)	> 32
<i>Candida parapsilosis</i> QC FTL strains	> 16
<i>Candida guilliermondii</i> (FTL strains) (3)	2– > 16
<i>Aspergillus fumigatus</i> (MDPL strain) (1)	8
<i>Aspergillus fumigatus</i> (FTL strains) (3)	> 16
<i>Rhizopus oryzae</i> (FTL strains) (3)	2
<i>Blastomyces dermatitis</i> (FTL strains) (10)	0.5–1
<i>Histoplasma capsulatum</i> (FTL strains) (10)	0.125–1
<i>Coccidioides</i> spp. (FTL strains) (10)	8–16
<i>Paecilomyces variotii</i> QC FTL strains	> 16

^a FTL strains, strains from the Fungus Testing Laboratory at the University of Texas Health Science Center at San Antonio; MDPL strains, strains from Maurizio Del Poeta's laboratory. S isolates, clinical isolates sensitive to fluconazole; R isolates, clinical isolates resistant to fluconazole; QC, quality control.

rial). BHBM was synergistic and D0 was additive when combined with tunicamycin. In contrast to fluconazole, *C. neoformans* cells did not develop resistance to either BHBM or D0 after 15 days of *in vitro* passages (120 generations) with a population size of 10^6 cells/ml (data not shown).

BHBM and D0 are fungicidal against intracellular *C. neoformans*. Since both BHBM and D0 exhibited fungicidal activity against *C. neoformans*, we examined their killing activity using a time-kill assay. BHBM showed concentration-dependent killing (Fig. 2A), whereas D0 showed time-dependent killing (Fig. 2B). BHBM is less inhibitory toward GlcCer synthesis compared to D0, and it is only at higher concentrations that its inhibitory action becomes comparable to that of D0 (Fig. 1). Thus, the dose response associated with BHBM might be directly related to its ability to inhibit GlcCer synthesis, resulting in increased fungicidal activity with increased GlcCer inhibition. *C. neoformans* is a facultative intracellular pathogen and is able to replicate within phagocytic cells, such as macrophages. Thus, the ability of BHBM to kill phagocytosed *C. neoformans* cells was also examined. The J774.16 macrophage cell line was infected with *C. neoformans* in the presence of opsonins. The opsonins and extracellular fungal cells were then washed off, and BHBM was added to test its activity against intracellular fungal cells. Analysis of CFU revealed that

BHBM significantly decreased the intracellular replication of *C. neoformans* inside macrophages. This effect was dose dependent, particularly after 12 and 24 h of incubation (Fig. 2C). Drugs showed little cytotoxic activity against the J774 cells with a 50% effective concentration (EC_{50}) of $50 \mu\text{g/ml}$ for both drugs (see Fig. S1 in the supplemental material), leading to a favorable EC_{50}/MIC_{80} selectivity index (50 for BHBM and >100 for D0). In addition, toxicity was also tested in A549 and L2 mammalian cell lines, and EC_{50} s of $112 \mu\text{g/ml}$ and $72 \mu\text{g/ml}$ were found for the two cell lines, respectively. These EC_{50} concentrations did not inhibit mammalian GlcCer synthesis (data not shown), suggesting that drug toxicity at these concentrations is not due to the inhibition of mammalian GlcCer.

BHBM and D0 have potent antifungal activity against cryptococcosis. The efficacy of BHBM and D0 was tested in mouse models of cryptococcosis. Treatment was initiated the same day that mice were infected intranasally with 5×10^5 *C. neoformans* cells with a drug concentration of 1.2 mg/kg of body weight/day. Most (90%) BHBM-treated mice and 70% of D0-treated mice survived *C. neoformans* infection for up to 60 days, whereas 100% of untreated mice died within 33 days ($P < 0.001$ for both BHBM- and D0-treated mice versus untreated mice) (Fig. 3A). The fungal burden in the lungs and brain were studied during the course of infection. Drug treatment significantly reduced the fungal burden in both organs, and no cells were detected in the brain tissue at the end of the study (see Fig. S2 in the supplemental material). It is possible that the drugs were able to act in the lungs or the bloodstream and prevent fungal dissemination to the brain. However, the total absence of fungal cells in the brain at later time points (Fig. S2B) suggests that perhaps the drugs may act directly in the brain tissue. Drugs did not show significant *in vivo* toxicity. Blood work of BHBM- and D0-treated mice after 60 days of treatment showed a slight but insignificant increase of liver aspartate amino-

TABLE 2 *In vitro* antifungal activities of BHBM determined by the percentage inhibition of ATP (IC_{50}) against *Pneumocystis murina* and *Pneumocystis jirovecii*^a

<i>Pneumocystis</i> isolates	BHBM IC_{50} ($\mu\text{g/ml}$) after exposure for:			
	24 h	48 h	72 h	96 h
<i>P. murina</i> HA isolates	1.02	<0.01	<0.01	2.02
<i>P. jirovecii</i> VM isolates	0.912	0.159	0.074	0.072

^a IC_{50} , 50% inhibitory concentration.

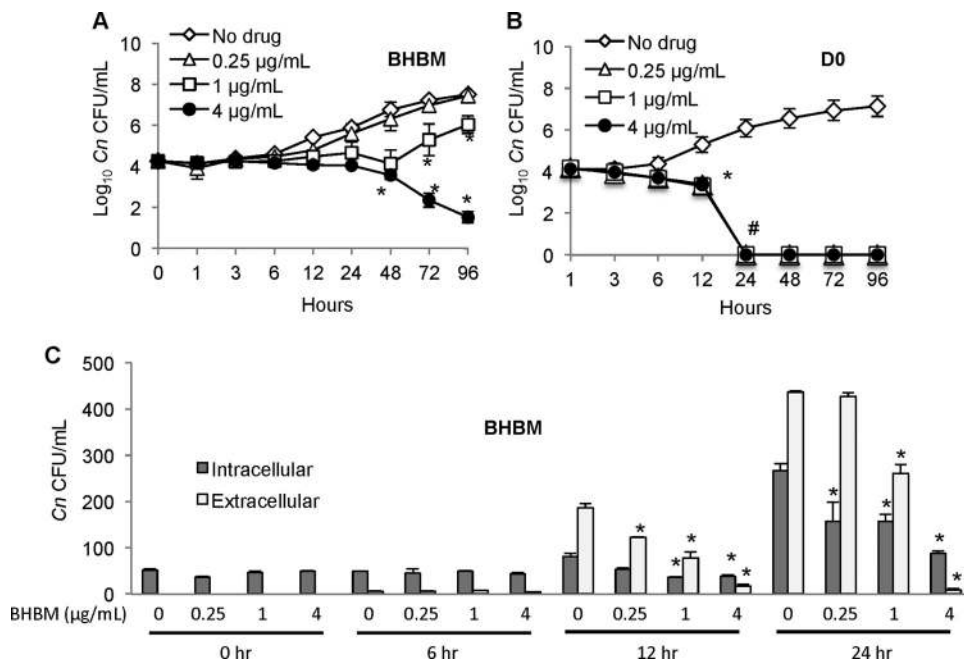


FIG 2 Killing activity of BHBH and D0. Killing activity was determined using an *in vitro* killing assay in which the compounds were added to *C. neoformans* cells, which were then incubated at 37°C, 5% CO₂, and pH 7.4. The number of CFU were counted during the 96-h incubation. (A and B) Both BHBH (A) and D0 (B) showed fungicidal activity. BHBH showed concentration-dependent killing, whereas D0 showed time-dependent killing. D0 is more effective in killing *C. neoformans* (100% dead cells within 24 h), and the killing activity does not occur earlier than 24 h with higher doses. BHBH kills more slowly, requiring at least 72 h of incubation to kill about 50% of the cells. Values that are significantly different are indicated as follows: *, $P < 0.05$ comparing treated cells versus untreated cells (no drug); #, $P < 0.001$ comparing treated cells versus untreated cells (no drug). (C) Intracellular activity of BHBH was assessed by incubating macrophages with internalized *C. neoformans* cells with different concentrations of BHBH in the absence of opsonins. Values that are significantly different are indicated as follows: *, $P < 0.05$ comparing extracellular or intracellular treated (0.25, 1, or 4 $\mu\text{g/ml}$) versus extracellular or intracellular untreated (0 $\mu\text{g/ml}$), respectively. Statistical analysis was performed using analysis of variance (ANOVA). Data were compiled from three independent experiments.

transferase (AST) (125 ± 75 U/liter) in BHBH-treated mice compared to untreated mice (50 ± 9 U/liter). All other blood parameters for liver and kidney function were normal, as were the number of erythrocytes, thrombocytes, and leukocytes.

Pharmacokinetic studies following BHBH treatment were performed in immunocompetent control healthy mice and immunosuppressed/infected (IS/IN) mice. In immunocompetent mice, the half-life of high-dose intravenous (i.v.) BHBH was 1.03 h. The half-lives of BHBH after low-dose and high-dose administration were 1.70 and 1.43 h, respectively (see Table S2 in the supplemental material). In infected mice, the half-lives of BHBH after low-dose and high-dose administration were 0.79 h and 0.84 h, respectively. The changes in the half-lives of the drugs between immunocompetent and immunosuppressed/infected animals are due to interactions between the drugs and corticosteroids used for immunosuppression; we have found that these drugs do not interact with another immunosuppressant, cyclophosphamide (data not shown).

A second mouse survival study was performed to test the efficacy of BHBH and D0 against invasive cryptococcal infection of the central nervous system (CNS). Fluconazole and amphotericin B were also included in these studies to compare the efficacies of these compounds to those of commonly used drugs. All mice in the vehicle-treated control group succumbed 7.0 ± 1.1 days postinfection. All drugs prolonged survival significantly compared with the control, although none of the drugs completely protected the mice from infection (Fig. 3B). BHBH- and D0-treated mice succumbed 11.1 ± 3.7 ($P < 0.05$ versus untreated

mice) and 10.5 ± 4.2 days ($P < 0.05$ versus untreated mice) postinfection, respectively. This was similar to the survival pattern observed with fluconazole, with an average survival of 10 ± 2 days postinfection ($P < 0.05$ versus untreated mice). Mice treated with amphotericin B succumbed at an average of 23.5 ± 6.5 days postinfection ($P < 0.005$ versus untreated mice).

BHBH and D0 have antifungal activity against pneumocystosis. BHBH showed marked *in vitro* activity against *P. murina* and *P. jirovecii*. Therefore, its *in vivo* activity in murine models of pneumocystosis was tested. Since establishment of lethal pneumocystosis in murine models requires immunosuppression, mice were treated with corticosteroids prior to infection. Four experimental groups of mice were included: (i) infected mice treated with vehicle (negative control), (ii) infected mice treated with trimethoprim-sulfamethoxazole (T/S), (iii) infected mice treated daily with BHBH (3.2 mg/kg), and (iv) infected mice treated with D0 (1.25 mg/kg/day). Mice treated with 3.2 mg/kg BHBH survived significantly longer than untreated mice did ($P < 0.05$) (Fig. 3C). D0 appeared to display some toxicity in mice immunosuppressed with corticosteroids. Thus, CD4⁺ cell depletion was used to induce immunosuppression in studies of D0 against pneumocystosis. In this model, 1.25 mg/kg/day of D0 significantly improved survival ($P < 0.05$) (Fig. 3C) with no apparent signs of toxicity. No significant differences were seen in the number of asci or nuclei in lung homogenates of the vehicle-treated negative control versus the BHBH treatment groups or the D0 treatment groups (see Fig. S2C to F in the supplemental material). There was a significant reduction in both asci and nuclei count following

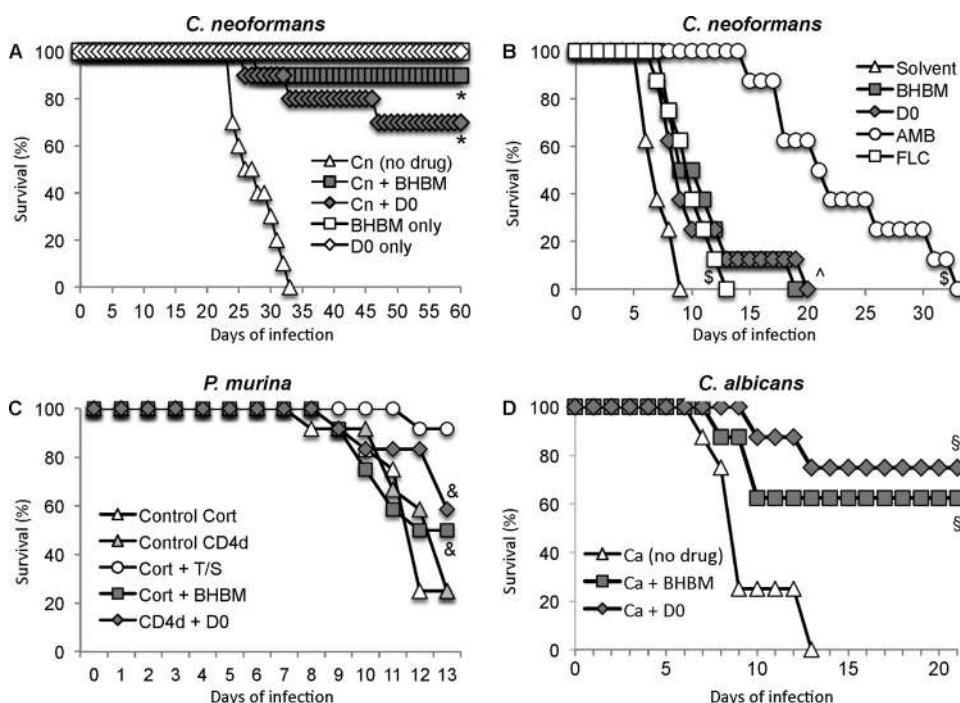


FIG 3 Effects of BHBM and D0 on survival of mice upon infection with *C. neoformans*, *P. murina*, or *C. albicans*. (A) Cryptococcosis. Mice were infected intranasally with *C. neoformans* (Cn) and received 1.2 mg/kg/day of either BHBM or D0 intraperitoneally (10 mice per group). Values that are significantly different are indicated as follows: *, $P < 0.001$ comparing BHBM- or D0-treated mice versus untreated mice (no drug). (B) Cryptococcosis. Survival of mice infected intravenously with *C. neoformans* (8 mice per group) and treated intraperitoneally either with BHBM, D0, fluconazole (FLC), or amphotericin B (AMB). Values that are significantly different are indicated as follows: ^, $P < 0.05$ comparing BHBM- or D0-treated mice versus untreated mice (solvent); \$, $P < 0.005$ comparing FLC-treated mice versus untreated mice and AMB-treated mice versus untreated mice. (C) Pneumocystosis. Survival of corticosteroid-immunosuppressed (Cort) or CD4-depleted (CD4d) mice infected intranasally with *P. murina* after 13 days of intraperitoneal treatment with BHBM (3.2 mg/kg/day), D0 (1.25 mg/kg/day), or trimethoprim-sulfamethoxazole (T/S) (12 mice per group). Values that are significantly different are indicated as follows: &, $P < 0.05$ comparing BHBM- or D0-treated mice versus respective untreated controls. (D) Candidiasis. Survival of mice infected with *C. albicans* SC 5314 (Ca) intravenously received no drug or 1.2 mg/kg/day of either BHBM or D0 intraperitoneally (8 mice per group). Values that are significantly different are indicated as follows: \$, $P < 0.01$ comparing BHBM- or D0-treated mice versus untreated mice. Statistical analysis for survival studies was performed using Kruskal-Wallis test and by Student-Newman-Keuls t test for multiple comparisons using INSTAT.

13 days of T/S treatment versus the negative control and versus BHBM groups (Fig. S2C and S2D).

BHBM and D0 have antifungal activity against invasive candidiasis. Most *Candida* spp. examined were resistant *in vitro* to both BHBM and D0. However, previous studies have shown that GlcCer is required for virulence through a mechanism other than facilitating growth at neutral/alkaline pH (8), which is the pH used in our library screening. *In vitro* treatment of *C. albicans* cells with BHBM inhibited GlcCer synthesis in a dose-dependent manner (data not shown). Thus, the efficacy of BHBM or D0 against invasive candidiasis was evaluated. Invasive candidiasis was established in CBA/J mice by intravenous injection with a lethal dose of 10^5 *C. albicans* cells. Treatment started the same day with either BHBM or D0 using the same dose regimens used to treat cryptococcosis. After 21 days of infection, 75% of mice treated with D0 and 62.5% of mice treated with BHBM were still alive, whereas all untreated mice had succumbed by day 13 (Fig. 3D).

BHBM and D0 target metabolism and/or transport of certain ceramide species used for synthesis of GlcCer. Since the initial screening had demonstrated that BHBM and D0 affect the synthesis of GlcCer, biochemical studies were performed by thin-layer chromatography (TLC) and mass spectrometry to understand the effects of drugs on the sphingolipid pathway. Lipid profiling by TLC revealed that BHBM treatment led to a decrease in

GlcCer levels and increased dihydroceramide, sphingosine, and sphingosine-1-phosphate (Fig. 4a). These changes were confirmed by mass spectrometry (Fig. 4b to e). Interestingly, the levels of C18 hydroxyceramide, the ceramide species that is a direct precursor of GlcCer, and its corresponding desaturated and methylated forms decreased upon BHBM (Fig. 4F to H) or D0 (data not shown) treatment, confirming a dysregulation of the ceramide synthesis upon treatment with BHBM. No significant changes in GlcCer levels were observed in mammalian cells after BHBM treatment at various time points (see Fig. S3 in the supplemental material).

BHBM affects fungal cell morphology and vesicular structure. The relationship between lipid composition and Golgi architecture is well established (15, 16). Thus, we set out to evaluate the effect of BHBM treatment on the Golgi accumulation of NBD C6-ceramide $\{N-[7-(4\text{-nitrobenzo-2-oxa-1,3-diazole})]-6\text{-aminocaproyl-D-erythro-sphingosine}\}$, indicating altered Golgi function. The peripheral distribution reported for *C. neoformans* was observed for NBD C6-ceramide staining in control cells; however, a substantial accumulation of this compound was detected in BHBM-treated yeasts of *C. neoformans* as observed by microscopy and confirmed by fluorescence-activated cell sorting (FACS) analysis (Fig. 5A and B). The majority of BHBM-treated yeasts displayed a ring accumulation of NBD C6-ceramide. Similar results

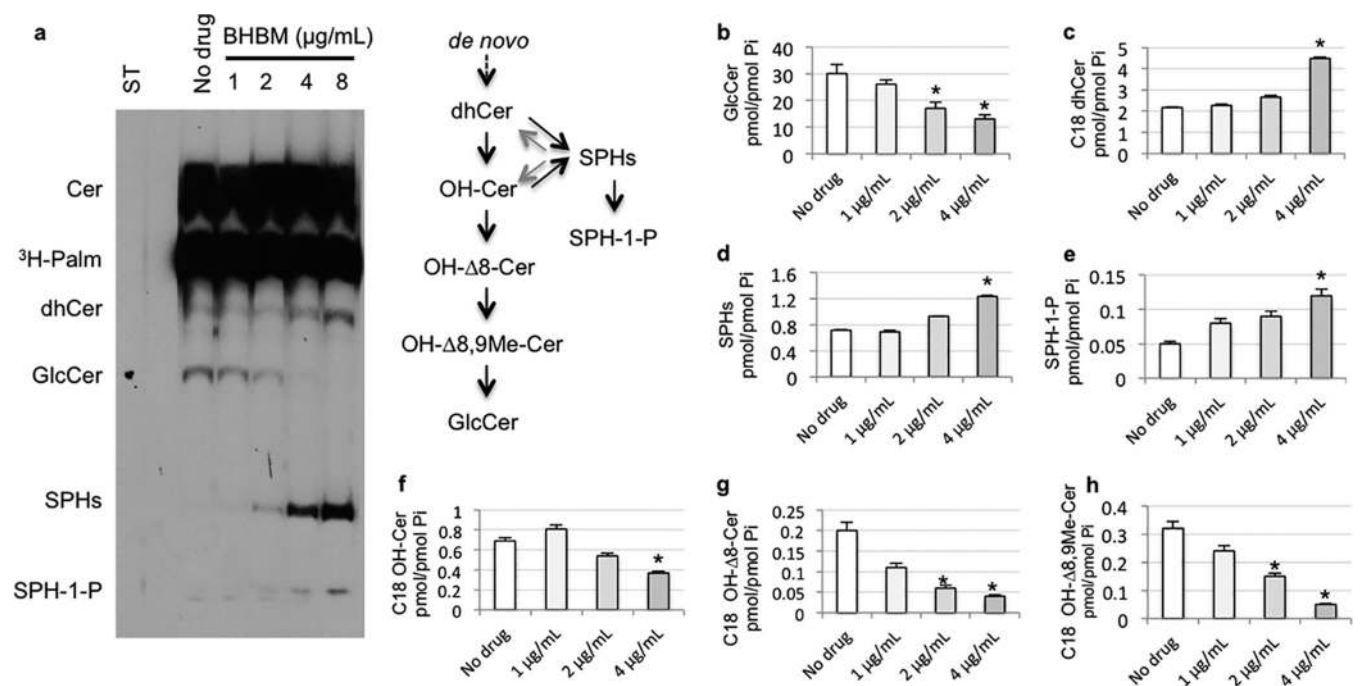


FIG 4 Measurements of sphingolipids upon treatment with BHBM. (a) Thin-layer chromatography analysis of sphingolipids (see diagram) isolated from untreated or BHBM-treated *C. neoformans* cells after *in vivo* labeling with [^3H]palmitate (^3H -Palm). (b to h) Lipid analysis by LC-MS. (b) C18 hydroxy ($\Delta 8$) 9 methyl-glucosylceramide (GlcCer); (c) C18 dihydroceramide (C18 dhCer); (d) sphingosine and dihydrosphingosine (SPHs); (e) sphingosine-1-phosphate and dihydrosphingosine-1-phosphate (SPH-1-P); (f) C18 hydroxyceramide (C18 OH-Cer); (g) C18 hydroxy $\Delta 8$ -ceramide (C18 OH- $\Delta 8$ -Cer); and (h) C18 hydroxy $\Delta 8$, 9 methyl-ceramide (C18 OH- $\Delta 8$, 9Me-Cer). Values that are significantly different are indicated as follows: *, $P < 0.05$ comparing treated to untreated (no drug). Statistical analysis was performed using analysis of variance (ANOVA) test. Statistical significance is accepted at a P value of < 0.05 . Data were compiled from three independent experiments.

were observed in *C. albicans*, confirming an altered distribution of NBD C6-ceramide after BHBM in hyphal forms. In addition, BHBM treatment significantly reduced the yeast-to-hypha differentiation in *C. albicans* (Fig. 5A). This defect in change of morphology might explain the loss of virulence in candidiasis (Fig. 3D), as *Candida* species that are locked in the yeast form are known to lose virulence (17). Additional fluorescent images are shown in Fig. S4 in the supplemental material.

Electron microscopy examination of drug-treated cells showed an accumulation of large vesicles inside the cells (Fig. 6A), while control cells maintained a regular organization and structure of intracellular vesicles (Fig. 6B). Vesicle accumulation in drug-treated cells was observed as single vesicles (Fig. 6A and D, arrows) and fused vesicles (Fig. 6A and D, arrowheads). Morphometric analysis revealed that there was a significant increase ($P < 0.05$) in the volume occupied by the intracellular vesicles in BHBM-treated cells (Fig. 6C). The numbers of vesicles per square micrometer of cell surface area were 0.84 ± 0.58 in BHBM-treated cells and 0.93 ± 0.54 in D0-treated cells compared to 0.33 ± 0.36 in untreated cells. The increase in both volume and number of intracellular vesicles suggests defects in secretion processes induced by the drug (Fig. 6C). In addition, plasma membrane-limited structures, which seemed to accumulate portions of the cytoplasm, were frequently seen accumulated in the periplasmic space (Fig. 6E). Transmission electron microscopy (TEM) images of D0-treated cells and additional images of BHBM-treated cells are presented in Fig. S5 in the supplemental material.

Cellular targets of BHBM. Two approaches were used to find the potential target(s) of BHBM. In the first approach, a *Saccha-*

romyces cerevisiae HIP-HOP (haploinsufficiency profilng-homozygous deletion profilng) assay comprising of essential genes as heterozygous diploids and nonessential genes as homozygous diploids (18) was screened to find the potential pathways affected by the drug. Of this genome-wide collection of 5,900 mutants, 23 were >2 -fold more sensitive to BHBM than the vehicle-treated control (see Table S3 in the supplemental material). Of these 23 genes, 8 were not considered further because they corresponded to dubious open reading frames or lacked any homology to *C. neoformans*. Among the remaining 15 significant sensitive genes, 9 genes (*RET2*, *UBP3*, *SEC26*, *PEP7*, *SEC31*, *YML018C*, *SNF8*, *GOS1*, and *RET3*) are involved in the regulation of vesicle sorting or transport between Golgi apparatus and endoplasmic reticulum (ER). This was in agreement with the observations of fungal cell morphology and vesicular structure after drug treatment (Fig. 5 and 6). These findings were also consistent with the decrease of GlcCer levels upon BHBM treatment, as vesicle transport is the main mechanism by which ceramide is transported between the ER and Golgi apparatus for the synthesis of GlcCer and other complex sphingolipids (19–21). These genes are conserved in *C. neoformans*, but they have not been characterized experimentally. The other six genes detected in the HIP-HOP screen (*MTW1*, *REG1*, *SPT4*, *SAP4*, *GLC7*, and *ACT1*) regulate chromatin organization, cell cycle progression, or cell division, functions that are known to be regulated by GlcCer (14, 22).

To pinpoint the cellular targets of BHBM, a second approach, generation of BHBM-resistant mutants, was followed. The drug-sensitive *S. cerevisiae* RYO0622 strain was used for the generation of mutants (23). A prescreening study exposing this strain to var-

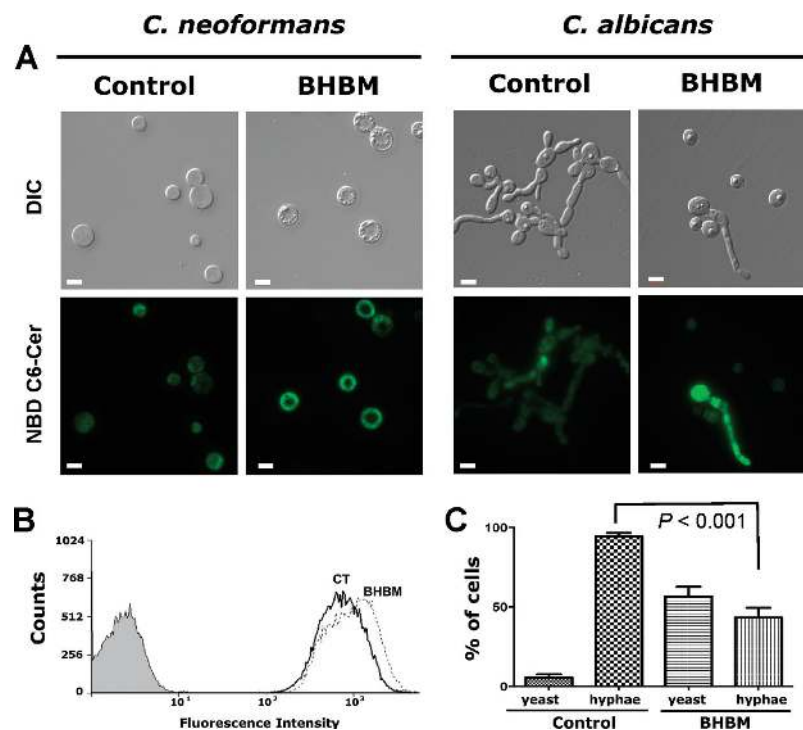


FIG 5 Effect of BHBM on Golgi morphology in *C. neoformans* and yeast-to-hyphal differentiation in *C. albicans*. (A) Control or BHBM-treated cells were stained with NBD C6-ceramide (Golgi and Golgi-derived compartments, green fluorescence). DIC, differential interference contrast; NBD-Cer, NBD 6-ceramide. Bars, 5 μm . (B) FACS analysis shows NBD C6-ceramide accumulation in *C. neoformans*. The gray histogram corresponds to *C. neoformans* yeast in the absence of NBD C6-ceramide. CT, control (no BHBM treatment). (C) Percentage of yeast and hyphal forms under control conditions and after BHBM treatment. Statistical analysis was performed using analysis of variance (ANOVA) test. Statistical significance is accepted at a P value of <0.05 . The images in panels A and B are representative of three separate experiments. The data in panel C were compiled from three independent experiments.

ious concentrations of BHBM revealed that a drug concentration of 133 $\mu\text{g}/\text{ml}$ completely inhibited yeast growth (100% inhibitory concentration [IC_{100}]). Incubating 10^6 cells of *S. cerevisiae* RYO0622 strain with BHBM at the IC_{100} resulted in seven resistant colonies, the genomes of which were sequenced and compared with the NCBI sacCer3 reference genome using the Genome Analysis Toolkit (GATK). This analysis led to the identification of mutations in four genes, *APL5*, *COS111*, *MKK1*, and *STE2*, that were present in all resistant mutants. The proteins encoded by these loci are known to be involved in vesicle trafficking, budding, and cell cycle progression (24–27), again in agreement with the observations of cell morphology and known phenotypes in the absence of GlcCer (14, 22). These findings also closely match the pathway proposed by the HIP-HOP analysis. Interestingly, these four genes each interact with UBI4 which encodes ubiquitin and which is conjugated to proteins to target them for degradation. UBI4 is a member of the endomembrane recycling pathways as defined by Finley et al. (28).

To confirm drug resistance, individual mutants along with the parent strain were grown in the presence of various concentrations of BHBM. Various concentrations of fluconazole and methyl methane sulfonate (MMS) were used as controls (Fig. 7). All individual mutants showed increased resistance to BHBM in the range of 11 to 92 $\mu\text{g}/\text{ml}$ (Fig. 7), while all mutants showed similar susceptibility to fluconazole and MMS. The increased re-

sistance of these mutants to BHBM treatment confirms that the above-mentioned genes are indeed the targets of BHBM, and the absence of these targets impairs the killing activity of the drug. It is worth noting that deep-sequencing analysis also revealed the presence of mutations in another gene, *SLA2*, that is also involved in vesicular transport (29). Although the Δsla2 mutant was not resistant to BHBM, it remains to be determined whether point mutations within the *SLA2* open reading frame do in fact confer resistance.

DISCUSSION

In this study, we have identified and characterized a new class of antifungal compounds, the hydrazycins (specifically BHBM and D0), which decrease the synthesis of fungal, but not mammalian, GlcCer. These compounds were effective against cryptococcosis, candidiasis, and pneumocystosis in animal models and target four genes involved in vesicular trafficking and cell budding. The compounds were well tolerated by animals and can potentially pave the way for the development of a new class of antifungals.

Both BHBM and D0 are acylhydrazone compounds with the structure $\text{R}_1\text{R}_2\text{C} = \text{NNH}_2$ (Fig. 1) (30–32). Hydrazone molecules have been shown to exert diverse biological functions, including antibacterial, antifungal, antiviral, antiparasitic, anticancer, and antidepressant effects (33–36), but these activities are linked to specific structures of hydrazones, which we can readily modify

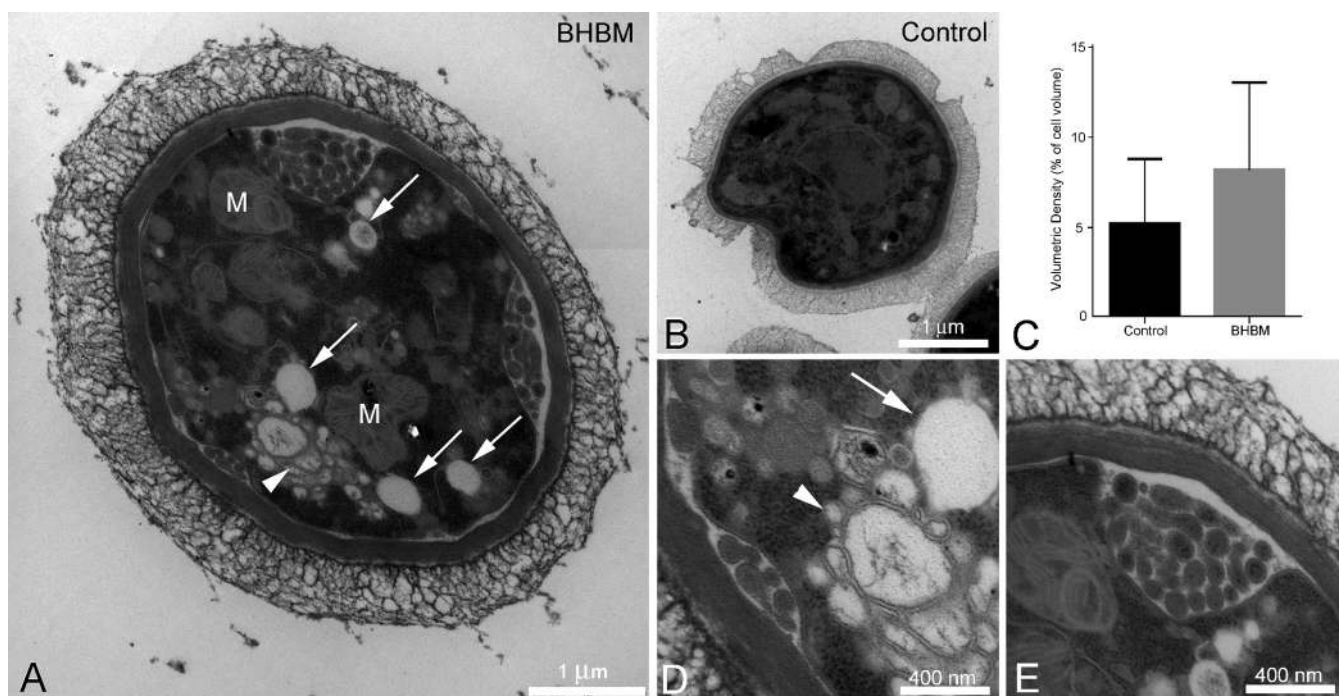


FIG 6 Transmission electron microscopy examination of high-pressure frozen and freeze substituted *C. neoformans* yeast cells. (A, D, and E) Cells treated with 4 $\mu\text{g}/\text{ml}$ of BHBM for 6 h, showing accumulation of intracellular vesicles (arrows) and regions containing a “reticulum” presumably formed by the fusion of intracellular vesicles (arrowheads). M, mitochondrion. (B) Control cells showing a regular aspect. (C) Morphometric analysis results showing the volumetric density of the intracellular vesicles in control and treated cells. (E) Accumulation of cytoplasm-rich vesicles in the periplasmic space. Images and data are representative of the results of three separate experiments.

(data not shown), potentially increasing their antifungal activity. Although previous literature exists on antimicrobial activity of hydrazone compounds, this is the first time that the ability of these compounds to block fungal GlcCer has been discovered.

BHBM and D0 exhibited antifungal activity against a variety of clinically relevant fungi (Table 1) and acted synergistically with currently available antifungal drugs (see Table S1 in the supplemental material). The ability of these compounds to exert fungicidal activity on phagocytosed *C. neoformans* cells is particularly important (Fig. 2). *C. neoformans* is able to survive and replicate inside macrophages (37), and replication inside nonactivated macrophages is an important factor in its pathogenicity (38). Furthermore, BHBM and D0 exhibited low cytotoxicity in a macro-

phage cell line (see Fig. S1 in the supplemental material) and a good selectivity index (EC_{50}/MIC ratio > 50), which is promising for their use as antifungals.

BHBM and D0 were effective against a variety of fungal infections *in vivo*. In mouse models of cryptococcosis, the drugs significantly increased the survival of mice that were infected with a lethal dose of *C. neoformans* via the intranasal route (Fig. 3A). Analysis of fungal burden demonstrated that drug treatment reduced the number of fungal cells in the brain throughout the course of the treatment, leading to the absence of fungal cells in the brain after 60 days (see Fig. S2 in the supplemental material). This observation indicates that drugs were able to reach the brain and clear the infection. This hypothesis is supported by the observa-

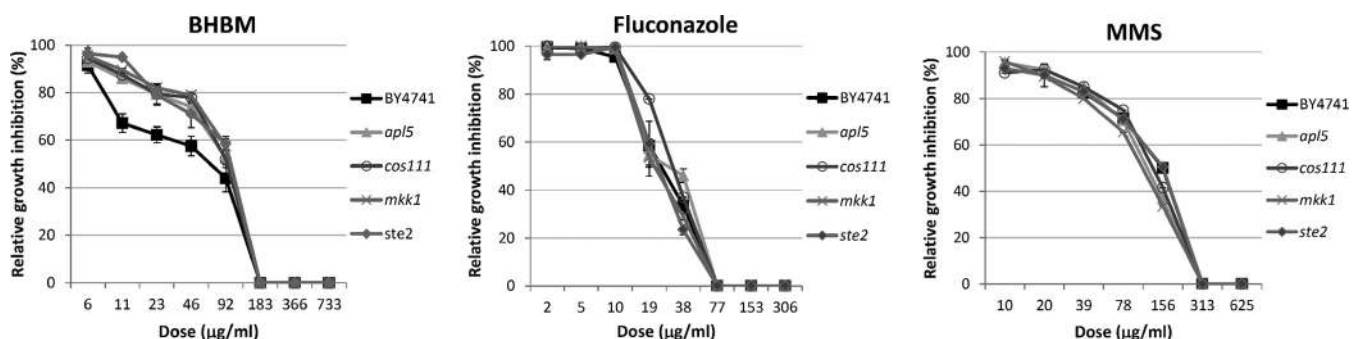


FIG 7 Effects of BHBM, fluconazole, and methyl methane sulfonate (MMS) on wild-type BY4741 and $\Delta apl5$, $\Delta cos111$, $\Delta mkk1$, and $\Delta ste2$ deletion strains. Relative growth inhibition was calculated by the average rate after normalizing the OD_{600} values in drug-treated wells against the DMSO control wells on each assay plate. The mutant strains show increased resistance to BHBM but not to fluconazole or MMS. Results are from two independent growth assays.

tion that BHBM is readily found in brain tissue upon administration (data not shown), and this tissue distribution may explain the low serum half-life and the effect on cryptococcal meningitis. In an aggressive model of cryptococcosis, in which the infection was established via tail vein injection, the drugs performed similarly to fluconazole in prolonging survival in our murine model (Fig. 3B). The concentration of fluconazole was almost eight times higher than that of BHBM and D0, suggesting that these drugs could be more effective than fluconazole. While amphotericin B was the most effective drug in this mode of infection, this drug is associated with drawbacks such as adverse reactions and nephrotoxicity (39, 40). BHBM and D0 are well tolerated by animals; thus, it is possible to augment their dose regimen for improved antifungal effect.

In addition to cryptococcosis, both drugs were effective in *in vivo* infection models of pneumocystosis and candidiasis (Fig. 3C and D). In the case of pneumocystosis, BHBM was able to increase survival in corticosteroid-treated mice, while D0 was effective in improving the survival of CD4-depleted mice. Although T/S was the most effective drug, this drug has significant side effects, and relapse and recurrence of infections are often observed when using secondary therapies (41). Thus, BHBM and D0 can potentially provide new options for pneumocystosis treatment. Previous studies have shown antifungal activity of fluconazole against *C. albicans* *in vivo* despite *in vitro* resistance (42). A similar phenomenon was observed with our drug compounds. It has been shown that GlcCer-deficient mutants in *C. albicans* lack the ability to cause virulence in the mouse model despite showing no growth defect *in vitro* (8). Thus, inhibition of GlcCer by BHBM and D0 is the likely mechanism for partially protecting the mice against invasive candidiasis.

Both BHBM and D0 inhibit the synthesis of GlcCer and significantly affect the levels of various sphingolipids (Fig. 4). However, GlcCer is not the only target of these drugs. Loss of GlcCer has a static effect on fungal growth (6), whereas BHBM and D0 are fungicidal. Interestingly, sphingosine species accumulate in fungal cells upon BHBM or D0 treatment (Fig. 4), a phenomenon that is not observed when the glucosylceramide synthase gene (*GCS1*) is deleted (5), and these sphingolipids are highly toxic. These sphingolipids do not significantly accumulate in mammalian cells treated with BHBM or D0 (see Fig. S3 in the supplemental material), and this may also explain the lack of toxicity in this system.

The results of HIP-HOP analysis provided an indication that the drugs affect the genes involved in vesicular transport, cell budding, and cell cycle progression. Of the 23 genes identified in this analysis, 9 were involved in the regulation of vesicle sorting or transport between Golgi apparatus and ER, and endocytosis and another 6 genes were involved in cell budding and cell cycle progression (see Table S3 in the supplemental material). These observations suggested that vesicular transport, cell division, and cell cycle progression are targeted by the drugs. This provided a potential target pathway, which was supported by the electron microscopy images showing an accumulation of intracellular vesicles (Fig. 6).

Further understanding of the drug targets was provided by generation of mutants resistant to BHBM. Mutations in four genes, *APL5*, *COS111*, *MKK1*, and *STE2*, were found in all seven colonies that showed resistance to BHBM. The corresponding single deletion mutants of each of these genes (from the yeast deletion collections [43]) showed increased resistance to BHBM, but no

difference in resistance to the unrelated drugs fluconazole or MMS (Fig. 7), confirming that these genes encode proteins that have a critical role in the cellular response to BHBM. Of these 4 genes, *APL5* plays an important role in vesicular transport and has been shown to be involved in cargo inclusion into vesicles during the secretory and endocytic pathways (44, 45). Furthermore, the *APL5* protein directly interacts with the *VPS3* and *GOS1*-encoded proteins, which were identified by the HIP-HOP assay (46, 47). Similarly, *MKK1* directly interacts with *RET2* and *RET3* identified by the HIP-HOP assay (48). *COS111* and *STE2* may also interact with genes identified by the HIP-HOP assay in a process mediated by ubiquitin (49–52). In fact, one of the genes identified by the HIP-HOP assay to be highly upregulated is *UBP3*, which encodes a ubiquitin-specific protease working together with *UBI4* to regulate protein degradation and endocytosis. In fact, *UBI4* physically interacts with all the genes identified by the HIP-HOP assay except *SPT4*, *SAP4*, *SNF8*, and *VPS3*. *UBI4* also interacts with all proteins identified by the deep-sequencing analysis. *UBP3* is also essential for the regulation of the *COPI* system (encoded by *RET2*, *RET3*, *SEC26*, and *SEC31*). Thus, *UBI4* may be involved in the regulation of endocytosis and vesicle transport by interacting with *RET2*, *RET3*, *UBP3*, *REG1*, *SEC26*, *SEC31*, and *PEP7*, all of which are genes identified by the HIP-HOP analysis. *UBI* may be a hub between the proteins identified by the deep-sequencing analysis and those identified by the HIP-HOP assay. Vesicular transport is the main mechanism by which ceramide is transported from the ER to the Golgi apparatus for the synthesis of *GlcCer*, which in turn regulates cell cycle progression (5, 9, 12). The results of deep-sequencing analysis suggest that the drug compounds inhibit a protein product in the endocytic/vesicle transport pathway that leads to the formation of *GlcCer*; this will strip the drug of its main target, leading to increased resistance.

In summary, we have identified hydrazone molecules (BHBM and D0) that exhibit potent antifungal activity through a specific inhibition of fungal *GlcCer*. These molecules exerted antifungal activity in the mouse models of cryptococcosis, pneumocystis, and candidiasis and were well tolerated by animals. BHBM and D0 also affected fungal cell morphology and vesicular trafficking. These molecules target four genes that are involved in vesicular secretion and cell cycle progression. To the best of our knowledge, this study marks the first drugs that act based on the inhibition of fungal *GlcCer*. Given the antifungal potency of these drugs, further studies are warranted for their preclinical and eventually clinical development.

MATERIALS AND METHODS

Strains, media, and reagents. A series of fungal clinical isolates and reference strains were used in this study, including *Cryptococcus neoformans* (strain H99), *Cryptococcus gattii*, *Candida albicans*, *Candida krusei*, *Candida glabrata*, *Candida parapsilosis*, *Candida guilliermondii*, *Aspergillus fumigatus*, *Rhizopus oryzae*, *Blastomyces dermatitidis*, *Histoplasma capsulatum*, *Coccidioides* spp., *Paecilomyces variotii*, *Pneumocystis murina*, *Pneumocystis jirovecii*, and *Saccharomyces cerevisiae*. These strains were obtained from existing collections at the Fungal Testing Laboratory (University of Texas Health Science Center at San Antonio, San Antonio), Del Poeta's laboratory (Stony Brook University), Cushion's laboratory (University of Cincinnati), and Nislow's laboratory (University of British Columbia). Yeast peptone dextrose (YPD), yeast nitrogen base (YNB), Luria-Bertani (LB), Roswell Park Memorial Institute (RPMI 1640), and Dulbecco's modified Eagle's medium (DMEM) were purchased from Invitrogen Life Technologies (Grand Island, NY). Fluconazole, amphotericin B, dexamethasone, cyclophosphamide, and tunicamycin were purchased from Sigma-Aldrich (St. Louis, MO). Caspofungin and posaconazole were obtained from Merck (Rahway, NJ). Voriconazole was obtained from Pfizer (Rey Brook, NY). *N'*-(3-bromo-4-hydroxybenzylidene)-2-methylbenzohydrazide (BHBM) and 3-bromo-*N'*-(3-bromo-4-hydroxybenzylidene) benzohydrazide (D0) were obtained from ChemBridge (San Diego, CA). Cryptococcal capsular monoclonal antibody MAb 18B7 was a gift from Arturo Casadevall's laboratory (Johns Hopkins University).

Library screening. The DIVERSet-CL library was obtained from ChemBridge (San Diego, CA) in a 96-well plate format and contained 10 mM compound per well in 100% dimethyl sulfoxide (DMSO). In each well, 10 compounds were mixed together. The compounds were first diluted to 1 mM each (1:10 dilution with 10% DMSO) with YNB medium buffered with HEPES at pH 7.4 containing 2% glucose and subsequently diluted to 300 μ M (1:3.3 dilution) with the same medium (3% DMSO). A 100- μ l aliquot of this solution was placed into each well of a 96-well plate and stored at -20°C until use. Then, 4×10^4 *C. neoformans* H99 cells in 100 μ l of YNB medium buffered at pH 7.4 with HEPES were added to each well. The final concentration of the tested drugs was 150 μ M in YNB medium containing 1.5% DMSO. The plates were incubated at 37°C in the presence of 5% CO_2 for 48 h. The optical density at 495 nm (OD_{495}) was recorded using the FilterMax 5 multimode microplate reader (Molecular Devices, Sunnyvale, CA). Compound cocktails showing an OD of $<80\%$ compared to the OD in the control well (1.5% DMSO but no drug) were selected for further studies.

Labeling of fungal cells with tritiated palmitate ($[^3\text{H}]$ palmitate). *C. neoformans* cells were grown in YNB (pH 7.4) at 37°C in the presence of 5% CO_2 for 16 h. The cells were centrifuged for 10 min at 3,000 rpm at room temperature. Supernatant was removed, and the cell pellet was suspended and counted. Next, 900 μ l containing 5×10^8 *C. neoformans* cells was placed into a 15-ml round-bottom Corning centrifuge tube. Then, 100- μ l volumes of different concentrations of BHBM or D0 diluted in YNB containing 0.1% DMSO were added, resulting in final concentrations of 0.25, 1, and 4 $\mu\text{g}/\text{ml}$ or 0.075, 0.3, and 1.2 $\mu\text{g}/\text{ml}$, respectively. The tubes were incubated in a shaker incubator at 225 rpm at 37°C in the presence of 5% CO_2 for 4 h. $[^3\text{H}]$ palmitate (30 $\mu\text{Ci}/\text{ml}$) (PerkinElmer, Waltham, MA) was added to the culture and incubated for an additional 2 h. Cells without the drug were included as a negative control. The cells were then pelleted, washed once with distilled sterile water, and resuspended in 1.5 ml of Mandala lipid extraction buffer. Lipids were extracted by the methods of Mandala et al. (53) and Blich and Dyer (54), followed by methanolic base hydrolysis as previously described. Extracted lipids were dried in an SPD210 SpeedVac system (Thermo Fisher Scientific). Dried lipids were resuspended in 30 μ l of 1:1 methanol-chloroform and loaded on thin-layer chromatography (TLC) silica gel 60 plates (EMD Millipore, Billerica, MA). Glucosylceramide (*GlcCer*) standard from soybean (Avanti Polar Lipids, Alabaster, AL) was added in a separate lane as a control. The sample was resolved in a tank containing chloroform-methanol-water (65:25:4) as the mobile phase. The TLC plates were then dried and exposed to iodine vapor for the identification of the *GlcCer* standard band, which was marked. The TLC plate was then enhanced by spraying with Enhancer (PerkinElmer) and exposed to X-ray film at -80°C for 72 h, after which the film was developed.

Labeling mammalian cells with tritiated palmitate ($[^3\text{H}]$ palmitate). The murine macrophage cell line J774.16 (ATCC) was maintained in DMEM containing 10% fetal bovine serum (FBS) and 1% penicillin-streptomycin (pen-strep) and were used until passage eight. Cells at a density of 5×10^6 cells/ml were cultured in a six-well culture plate for 14 h to achieve adherence. BHBM or D0 at the same concentrations used for fungal cells (see above) was added to the plate for 4 h. Then, 30 $\mu\text{Ci}/\text{ml}$ of $[^3\text{H}]$ palmitic acid was added, and the plate was further incubated for 2 h. Labeled, untreated J774.16 cells were included as a control. The cells were harvested by adding 0.05% trypsin-EDTA and scraping with a cell scraper, and then the cells were washed once with phosphate-buffered saline (PBS)

and dissolved in 2 ml methanol and 1 ml chloroform. Lipids were extracted by the method of Bligh and Dyer (54) followed by base hydrolysis. Lipid samples were dried in a SpeedVac vacuum concentrator, suspended in 30 μ l of 1:1 methanol-chloroform, and loaded on a TLC plate with GlcCer as the standard.

In vitro susceptibility testing. MICs were determined following the methods of the Clinical and Laboratory Standards Institutes (CLSI) with modifications. RPMI 1640 or YNB medium (pH 7.0, 0.2% glucose) buffered with HEPES was used for MIC studies. HEPES was used instead of morpholinepropanesulfonic acid (MOPS), because MOPS was found to inhibit the activity of BHBH and D0. BHBH and D0 were serially diluted from 32 to 0.03 μ g/ml or 19 to 0.02 μ g/ml, respectively, in a 96-well plate with the respective medium. The inoculum was prepared as described in the CLSI protocol M27-A3 guidelines (55). The plates were incubated at 37°C with 5% CO₂ for 24 to 96 h. The MICs were determined as the lowest concentration of the drug that inhibited 50% of growth compared to the control. The minimum fungicidal concentration (MFC) was also determined by taking 100 μ l of serial dilutions from each well, spreading it on YPD agar plates, and counting the CFU. MFC was defined as the lowest drug concentration that yielded three or fewer colonies (i.e., 99% of the inoculum was killed).

In vitro killing assay. *C. neoformans* cells from a culture grown overnight were washed in PBS and resuspended in YNB buffered with HEPES at pH 7.4. The cells were counted, and 2 \times 10⁴ cells were incubated with 1, 2, or 4 μ g/ml of BHBH or D0 in a final volume of 10 ml with a final concentration of 0.4% DMSO. The tubes were then incubated at 37°C with 5% CO₂ on a rotary shaker at 200 rpm. Aliquots were taken at time points and diluted, and 100- μ l portions were plated onto YPD plates. YPD plates were incubated in a 30°C incubator and after 72 h, the numbers of CFU were counted and recorded.

In vitro testing against *P. murina* and *P. jirovecii*. A characterized *P. carinii* strain isolated from rat lung tissue was distributed into triplicate wells of 48-well plates with a final volume of 500 μ l and a final concentration of 5 \times 10⁷ nuclei/ml. The cells were incubated with either 0.1, 1, 10, or 100 μ g/ml of BHBH or D0. The negative controls were media alone and ampicillin 10 μ g/ml, and the positive control was pentamidine isethionate at 1 μ g/ml. At 24, 48, and 72 h, 10% of the well volume was removed, and the ATP content was measured using PerkinElmer ATP-liteM luciferin-luciferase assay. The luminescence generated by the ATP content of the samples was measured by using a spectrophotometer (PolarStar Optima BMG, Ortenburg, Germany). Reduction in ATP consumption by *Pneumocystis* cells was considered a measure of drug efficacy. For a control for toxicity, ATP consumption was also measured in A549 and L2 mammalian cells. A sample of each group was examined microscopically on the final day of the assay to rule out the presence of bacterial contamination.

Intracellular effect of BHBH. To assess whether BHBH would be effective against intracellular *C. neoformans*, J774.16 macrophage cells were incubated with *C. neoformans* cells at a 1:1 ratio in the presence of opsonins (complement and antibody MAb 18B7 against the cryptococcal capsular antigen). After 2 h of incubation, about 60 to 80% of macrophages had at least one *C. neoformans* cell internalized. At this time, wells were washed to remove extracellular fungal cells and fresh DMEM with different concentrations of BHBH was added to each well. The plates were incubated at 37°C with 5% CO₂. At 0, 6, 12, and 24 h, extracellular cells were collected by washing and plated onto YPD agar plates for counting the CFU of extracellular cells. Macrophages were also lysed and plated onto YPD agar plates for counting the CFU of intracellular fungal cells.

Synergism assay. Synergistic activity was assayed by calculating the fractional inhibitory index (FIC). Briefly, in a 96-well plate, drug A (either BHBH or D0) was serially diluted from 16 to 0.015 μ g/ml (11 dilutions), whereas drug B (either fluconazole, amphotericin B, caspofungin, or tunicamycin) was serially diluted from 12 to 0.19 μ g/ml, 5 to 0.078 μ g/ml, 70 to 1.09 μ g/ml, and 6 to 0.09 μ g/ml (seven dilutions), respectively. The FIC was defined as (MIC combined/MIC drug A alone) + (MIC com-

bined/MIC drug B alone). Synergism was categorized as follows: strongly synergistic effect, FIC < 0.5; synergistic effect, FIC < 1; additive effect, FIC = 1; no effect, 1 < FIC < 2; antagonistic effect, FIC > 2.

In vitro toxicity. The murine macrophage cell line J774.16 was maintained in DMEM containing 10% FBS and 1% pen-strep. At passage 7, 10⁵ cells/well in DMEM containing 10% FBS were transferred into 96-well plates and cultured for 14 h for the cells to adhere to the wells. BHBH or D0 was added to the cells at concentrations ranging from 0.1 to 100 μ g/ml. The wells without the drug served as controls. The plate was incubated at 37°C with 5% CO₂. After 24 or 48 h, the supernatant was removed, and 50 μ l of 5-mg/ml 3-(4,5-dimethylthiazol-2-yl)-2,5-diphenyltetrazolium bromide (MTT) solution in PBS was added to each well. The plates were incubated for an additional 4 h. The formazan crystal formed inside the cell was dissolved by adding 50 μ l of isopropanol containing 0.1 N HCl. The optical density was measured at 570 nm.

Animal studies for cryptococcosis. Survival studies were performed with two routes of infection, intranasal and intravenous (i.v.) (tail vein). For survival studies with intranasal infection, 4-week-old CBA/J female mice (Jackson Laboratory, Bar Harbor, ME) were used. Ten mice per treatment or control group were evaluated. Mice were infected by nasal inoculation of 20 μ l containing 5 \times 10⁵ cells of *C. neoformans*. Treated mice received an intraperitoneal (i.p.) injection of 1.2 mg/kg of body weight/day of either BHBH or D0 in a final volume of 100 μ l of PBS containing 0.4% DMSO (PBS–0.4% DMSO) 2 h after receiving the inoculum. Untreated mice received 100 μ l of PBS–0.4% DMSO. Mice were fed *ad libitum* and monitored closely for signs of discomfort and meningitis. Mice showing abnormal gait, lethargy, tremor, significant loss of body weight, or inability to reach water or food were sacrificed, and survival was counted until that day. At the end of the survival study, tissue burden culture was performed in mice that survived the infection. Mice were sacrificed and their organs were extracted and homogenized in 10 ml sterile PBS using a homogenizer (Stomacher80; Cole-Parmer, Vernon Hills, IL). Organ homogenates were serially diluted 1:10 in PBS, and 100- μ l portions were plated on YPD agar plates and incubated at 30°C for 72 h for CFU count.

For survival studies using the intravenous injection of *C. neoformans*, 4-week-old CBA/J female mice (Jackson Laboratory, Bar Harbor, ME) were used. A total of 40 mice were infected by tail vein injection of 200 μ l containing 10⁵ cells of *C. neoformans* cells and were randomly separated into five groups (eight mice per group). The treated mice received an intraperitoneal injection of 1.2 mg/kg/day of BHBH, D0, or amphotericin B or 10 mg/kg/day of fluconazole in a final volume of 100 μ l of PBS containing 0.4% DMSO a few hours after receiving the inoculum. Untreated mice received 100 μ l of PBS–0.4% DMSO. Mice were fed *ad libitum* and monitored closely for signs of discomfort and meningitis. Mice showing abnormal gait, lethargy, tremor, significant loss of body weight, or inability to reach water or food were sacrificed, and survival was counted until that day.

Animal studies for pneumocystosis. For survival studies, 4- to 6-week-old C3H/HeN mice from the National Cancer Institute (Bethesda, MD) were used. Mice were infected with *P. murina* through exposure to mice with a fulminant *P. murina* infection (seed mice). These mice were immunosuppressed by the addition of 4 mg/liter dexamethasone to the drinking water. One milliliter of sulfuric acid was also added per liter of drinking water for disinfection. The seed mice were rotated within the cages for 2 weeks and then removed. After the mice had developed a moderate infection level (approximately 5 weeks), they were divided into groups containing 12 mice each: negative-control (control steroid), positive-control (trimethoprim-sulfamethoxazole [T/S]), BHBH-treated, and D0-treated groups. BHBH or D0 was administered intraperitoneally or by oral gavage on a milligram/kilogram/day basis for up to 3 weeks. Treatment was initiated after the mice developed infection. The dose, route, and frequency of administration varied depending on the agent being tested. At the end of the treatment, mice were sacrificed and processed for analysis. Slides were made from the lung homogenates at

different dilutions and stained with Diff-Quik to quantify the trophic forms and cresyl echt violet to quantify the asci. An additional group of 12 mice was selectively depleted of their CD4⁺ lymphocytes by antibody treatment with 300 μ g of GK 1.5 antibody (Biovest International, Minneapolis, MN) administered intraperitoneally three times on days 1, 3, and 7. After this initial treatment, the mice were infected by exposure to *P. murina*-infected mice. Mice were then treated with 100 μ g of GK 1.5 antibody intraperitoneally once a week for 6 weeks. After this, mice were treated with 1.25 or 12.5 mg/kg/day of D0 for 14 days while continuing the GK 1.5 treatment. Control mice received vehicle.

Animal studies for candidiasis. For survival studies, 8-week-old CBA/J female mice (Jackson Laboratory) were used. Eight mice per treatment or control group were evaluated. Mice were infected by intravenous inoculation of 100 μ l containing 10⁵ cells of *C. albicans* strain SC-5314. Treated mice received an intraperitoneal injection of 1.2 mg/kg/day of either BHBM or D0 in a final volume of 100 μ l of PBS containing 0.4% DMSO immediately after receiving the *Candida* inoculum. Untreated mice received 100 μ l of PBS–0.4% DMSO. Mice were fed *ad libitum* and monitored closely for signs of discomfort. At the end of the survival study, tissue burden culture was performed in mice that survived the infection. Mice were sacrificed, and their organs were extracted and homogenized in 10 ml sterile PBS using a homogenizer. Organ homogenates were diluted 10 times in PBS, and 100- μ l portions were plated on YPD agar plates and incubated at 30°C for 72 h for CFU count.

In vivo toxicity. Mouse toxicity studies were performed using 4-week-old CBA/J female mice from Jackson Laboratory. Five mice received 1.2 mg/kg/day BHBM for 60 days. Three control mice received a solvent injection per day. At day 60, blood was collected in two tubes: one with K₂EDTA and the other without K₂EDTA to allow blood clotting. The blood clot was then centrifuged at 1,500 rpm for 10 min, and the serum was collected and analyzed for liver and kidney blood tests. The noncoagulated blood was used for hematocrit and blood cell analysis. These tests were done using MASCOT HEMAVET 950FS (Drew Scientific Group, Düsseldorf, Germany).

Pharmacokinetics of BHBM. BHBM was dissolved in a mixture of cremophore-ethanol (1:1) to prepare a 10 mg/ml stock solution. The stock solution was diluted in PBS to obtain 200 μ g/ml and 400 μ g/ml solutions for i.v. and i.p. administrations in C3H/HeN mice ($n = 3$). BHBM was administered to control (healthy) mice or immunocompromised mice infected with *P. murina* at doses of 0.8 mg/kg and 1.6 mg/kg via tail vein injection or intraperitoneal injection in a final volume of 100 μ l. The mice were sacrificed, and blood samples were collected pre-dose and 0.5, 1, 2, 4, 8, 12, and 24 h after administration into K₂EDTA-containing tubes. The samples were centrifuged immediately, and plasma was collected and stored at –80°C until analysis. Plasma samples were extracted using methylene chloride. Briefly, 50 μ l of the plasma sample was taken into a glass vial, and 10 μ l of internal standard *N'*-(3-bromobenzylidene)-4-hydroxybenzohydrazide was added. After the contents of the glass vial were mixed, 1 ml of methylene chloride was added to the vial, and the samples were vortex mixed for 30 s followed by centrifugation for 5 min. Then, 800 μ l of supernatant was transferred to another tube and evaporated to dryness using a centrifugal evaporator. The residue was reconstituted in 100 μ l acetonitrile-water (50:50) solution, mixed, and transferred to mass spectrometry vials. Separation was performed under isocratic reverse-phase chromatographic conditions using a Waters XBridge C₁₈ column (3.5 μ m; 2.1 \times 100 mm) (Waters, Milford, MA), a Finnigan Surveyor MS pump (Thermo Fisher Scientific), and a Finnigan Micro AS autosampler (Thermo Fisher Scientific). The mobile phase consisted of water-acetonitrile with 0.1% formic acid (50:50) run at a flow rate of 200 μ l/min. Then, 5 μ l aliquots were analyzed using LTQ-FT liquid chromatography/tandem mass spectrometer (LC/MS/MS) with electrospray source in the positive ion mode (Thermo Fisher Scientific). The retention time of BHBM was 5.7 min. The lower limit of quantification (LLOQ) was 10 ng/ml. Systemic exposure of BHBM in mice was quantified by calculating the area under the concentration-time curve

(AUC) of the drug from predose to the end of the dosing interval (AUC_{0–t}) using the linear trapezoidal rule by noncompartmental analysis employing Phoenix WinNonlin 6.3 (Pharsight Corp., Mountain View, California). The half-life ($t_{1/2}$) was calculated as 0.693/ λ_z , where λ_z is the terminal elimination rate constant. Bioavailability of the intraperitoneal route was calculated for each group as the dose-normalized ratio of AUC_{0–t} between the intraperitoneal route (0.8- or 1.6-mg/kg dose) and intravenous route (1.6-mg/kg dose).

Lipid mass spectrometry. For lipid analysis by mass spectrometry, fungal cells (*C. neoformans* H99 or *C. albicans* SC-5314) were grown in YNB and incubated with BHBM or D0 as explained above for *in vivo* labeling (except that tritiated palmitate was not added) for 6 h. Samples without drug were included as a control. Before lipid extraction, lipid internal standards (C17 ceramide and C17 sphingosine) were added. Lipids were then extracted, and one-fourth of the sample was aliquoted for determination of the inorganic phosphate. The remainder of the sample was subjected to base hydrolysis and then analyzed using LC-MS as previously described (6). Results were normalized using the inorganic phosphate levels.

NBD C6-ceramide staining. The Golgi apparatus of *C. neoformans* H99 and *C. albicans* SC-5314 was stained with NBD C6-ceramide {N-[7-(4-nitrobenzo-2-oxa-1,3-diazole)]-6-aminocaproyl-D-erythro-sphingosine} based on the property that this fluorescent lipid accumulates at the Golgi apparatus of either living or fixed cells. Control or BHBM-treated (4 μ g/ml) yeast cells were fixed with 4% paraformaldehyde in PBS. Cell suspensions were then washed with the same buffer and incubated with NBD C6-ceramide (20 mM) for 16 h at 4°C. The cells were then incubated with bovine serum albumin (BSA) (1%) at 4°C for 1 h to remove excess NBD C6-ceramide. After the cells were washed with PBS, they were incubated with 10 μ g/ml 4',6-diamidino-2-phenylindole (DAPI) (Sigma-Aldrich, St. Louis, MO, USA) for 30 min at room temperature. The cells were washed with PBS, and stained cell suspensions were mounted over glass slides as described above and analyzed using an Axioplan 2 microscope (Zeiss, Germany). Fluorescence intensity of yeasts labeled with NBD C6-ceramide were compared using a FACScan flow cytometer (BD Biosciences, Franklin Lakes, NJ). A histogram with the total number of events and fluorescence intensity was prepared. Unlabeled cells were used as a negative control (56). To determine whether BHBM is able to inhibit *C. albicans* differentiation, the numbers of yeast and hyphal forms were counted after BHBM treatment and compared with control conditions in the absence of drug. Twenty random fields (approximately 120 cells) were analyzed.

TEM. Transmission electron microscopy (TEM) analysis was performed using two methods. In the first method, the samples were prepared by the procedure of Heung et al. (57) (with minor modifications) and were used for rough imaging and vacuole counting. In the second method, the samples were prepared using high-pressure freezing (HPF) and were used for high-quality imaging and estimation of the cell surface area occupied by the vacuoles. In the first method, *C. neoformans* cells were grown in YNB (pH 7.4) at 37°C with 5% CO₂ and treated for 6 h with either BHBM or D0 (4 μ g/ml). Untreated cells were included as a control. The cells were pelleted at 3,000 rpm (1,700 \times g) and fixed with 2% electron microscopy (EM)-grade glutaraldehyde in PBS solution for 1 h. Samples were then washed in PBS, placed in 1% osmium tetroxide in 0.1 M PBS, dehydrated in a graded series of ethyl alcohol, and embedded in Embed812 resin. Ultrathin 8-nm sections were cut with a Leica EM UC7 ultramicrotome (Leica Microsystems Inc., Buffalo Grove, IL) and placed on uncoated mesh copper grids. The sections were then counterstained with uranyl acetate and lead citrate and viewed with a FEI Tecnai12 BioTwinG2 electron microscope (FEI, Hillsboro, OR). Digital images were acquired with an AMT XR-60 charge-coupled-device (CCD) digital camera system.

In the second method, cells were treated with BHBM for the same amount of time. For HPF, BHBM-treated and control cells were centrifuged at 1,500 \times g for 5 min, and the pellet was sandwiched between

aluminum specimen carriers (3 × 0.5 mm) (Bal-Tec Corp., Liechtenstein). This pellet was placed between two types of specimen carriers (type B1 and B2) so that the cells were protected in a 200- μ m cavity on one carrier. The pellet was also inserted by capillary action in 2-mm pieces of 200- μ m-diameter cellulose capillaries, and one end of the capillary was closed using tweezers. Four capillaries were mounted between the two specimen carriers. The cavities were filled with hexadecane to avoid air entrance between the capillaries. The sandwiched samples were mounted in the HPF holder and frozen using a Bal-Tec HPM 010 or HPM100 high-pressure freezing machine (Bal-Tec Corp., Liechtenstein). After freezing, the samples were stored in liquid nitrogen. For embedding, the samples were carefully removed from the liquid nitrogen and immersed in medium consisting of 2% osmium tetroxide, 0.1% glutaraldehyde, and 1% water in acetone, precooled to -90°C using a Leica EMP apparatus. The samples were kept at -80°C for 72 h, then transferred to -20°C for 15 h, and maintained at 4°C for 2 h. The samples were then washed three times with acetone at room temperature and then embedded in Spurr's resin. Spurr's resin was polymerized at 70°C for 72 h. Sections of 70 nm were obtained, collected on 300-mesh copper grids, and poststained with uranyl acetate and lead citrate for conventional observation in a Zeiss 900 transmission electron microscope equipped with a Megaview III camera operating at 80 kV. For analysis of vesicle volumetric density, images of at least 30 cells from control and treated groups were acquired and measured. The total area of the cell and the area of intracellular vesicles were measured, and the percentage of cell volume occupied by these vesicles was estimated according to the Delesse principle. Statistical significance was determined by Student's *t* test. *P* values of <0.05 were considered statistically significant.

HIP-HOP library screening. The yeast deletion collection is comprised of approximately 5,900 individually bar-coded heterozygous diploid strains (HIP [haploinsufficiency profiling]) and ~4,800 homozygous diploid strains (HOP [homozygous deletion profiling]) (58). Pools of approximately equal strain abundance were generated by robotically pinning (S and P Robotics, Ontario, Canada) each strain (from frozen stocks) onto YPD agar plates as arrays of 384 strains/plate. After 2 days of growth at 30°C , colonies were collected from plates by flooding with YPD, and cells were adjusted to an optical density at 600 nm (OD_{600}) of 2. The fitness of each strain in each experimental pool was assessed as described previously (58). The BHBM dose that resulted in 15% growth inhibition in *S. cerevisiae* BY4743 (the parent strain of the yeast deletion collection) was determined by analyzing dose response over the course of 16 h of growth at 30°C . Screens of the homozygous deletion collection were performed for 5 generations of growth in BHBM, and screens of the heterozygous deletion collection were collected after 20 generations of growth. Cells were processed as described previously (59). Genomic DNA was extracted from each sample and subjected to PCR to amplify the unique bar code identifiers. The abundance of each bar code was determined by quantifying the microarray signal as previously described. A ranked list of all genes in the genome was generated for each experiment and then compared using gene set enrichment analysis (GSEA).

Generation of BHBM-resistant strains. For the generation of BHBM-resistant strains, the drug-sensitive *S. cerevisiae* RYO0622 haploid strain was used (23). Prescreening studies were performed to determine the IC_{100} dose of BHBM for this strain (the 100% inhibitory concentration [IC_{100}] at which 100% yeast cell growth is inhibited upon drug exposure). For this screening, 20 μl of RYO0622 cells (at an OD_{600} of 10^{-4}) were plated on solid synthetic complete (SC) medium alone or with DMSO or with various BHBM concentrations (67, 133, 266, 533, and 1,066 $\mu\text{g}/\text{ml}$) in a 48-well plate. The plates were incubated for 2 days at 30°C in the dark. These studies revealed an IC_{100} dose of 133 $\mu\text{g}/\text{ml}$.

Screening for the BHBM-resistant mutants was performed by growing the RYO0622 cells to mid-log phase (OD_{600} of ~ 0.5) in liquid SC medium before adjusting the cell density to 1×10^6 cells/ml (equivalent to an OD_{600} of ~ 0.1). One milliliter of cells was plated on solid SC medium containing DMSO solvent control (0.26% [vol/vol]) or BHBM

(133 $\mu\text{g}/\text{ml}$ IC_{100} dose) and incubated at 30°C in the dark. A lawn of cells grew on the solvent control, while seven BHBM-resistant colonies were identified after 9 days. Longer incubation did not result in the appearance of further resistant colonies. To confirm BHBM resistance, single colonies isolated from the BHBM-containing SC medium were plated onto fresh solid SC medium containing 133 $\mu\text{g}/\text{ml}$ BHBM and incubated for 2 days at 30°C in the dark. Robust BHBM-resistant cells were seen.

Next-generation sequencing of BHBM-resistant strains. Genomic DNA was extracted from RYO0622 and BHBM-resistant cells using a standard yeast DNA extraction protocol (60). Genomic DNA samples were quantified using Qubit fluorometry (Life Technologies) and diluted for sequencing library preparation using a Nextera XT library preparation kit according to the manufacturer's instructions (Illumina, San Diego, CA). For the initial round of sequencing, individual sequencing libraries were prepared for the parent and a single BHBM-resistant clone. These libraries were pooled and sequenced on a single MiSeq lane (Illumina), generating paired-end 150-bp reads. Further BHBM-resistant colonies were obtained in a second screen, and their DNAs were pooled at equal concentrations before preparation of a single sequencing library for the pool. This pool was sequenced alongside a new library for the parent strain on a single HiSeq 2500 lane (Illumina), generating paired-end 100-bp reads.

Mapping and variant calling. Raw FASTQ paired-end reads for the parent (RYO0622) and the BHBM-resistant pool were independently aligned to the NCBI *sacCer3* reference genome (genbank/genomes/eukaryotes/fungi/saccharomyces_cerevisiae/saccer_apr2011 at <http://hgdownload-test.cse.ucsc.edu/goldenPath/sacCer3/bigZips/>) using *bwa mem* v0.7.4-r385 (61) with the $-M$ flag to mark shorter split hits as secondary for compatibility with Picard. Resultant SAM files were converted to BAM format using *samtools* v1.1 and sorted by coordinate using *Picard* v1.96 (SortSam) (<http://picard.sourceforge.net>). PCR duplicate reads were filtered out using *Picard* MarkDuplicates and indexed using *Picard* BuildBamIndex. To call single nucleotide variants (SNVs), the GATK Unified Genotyper v2.1-8 (62) was run with the NCBI *sacCer3* reference genome, *stand_call_conf*=30, and *stand_emit_conf*=10 (63). The ploidy parameter was set at 1, since the parent and resistant strains are in haploid state. Realignment around known indels and quality score recalibration was not performed, since a database of known indels and known single nucleotide polymorphisms (SNPs) is not available.

Validation of BHBM-resistant yeast mutants. Four yeast genes (*ALP5*, *COS111*, *MKK1*, and *STE2*) were selected based on the high-quality variant calls present in the BHBM-resistant pool. To confirm BHBM resistance, the individual haploid Δapl5 , Δcos111 , Δmkk1 and Δste2 deletion mutants were assayed for growth fitness after treatment with BHBM. Unrelated drug controls, including methyl methane sulfonate (MMS) (cytotoxic) and fluconazole (antifungal) were assayed in parallel. Strains were cultured to mid-log phase (OD_{600} of ~ 0.5) in liquid YPD medium before adjusting the cell density to an OD_{600} of 0.0625 with YPD medium. The cells were transferred to 96-well plates containing 100 μl of YPD with DMSO solvent control (2% [vol/vol]), BHBM (6 to 733 $\mu\text{g}/\text{ml}$), MMS (10 $\mu\text{g}/\text{ml}$ to 625 $\mu\text{g}/\text{ml}$), or fluconazole (2 to 306 $\mu\text{g}/\text{ml}$) and incubated at 30°C for 24 h. The fitness of individual strains was measured using a spectrophotometer plate reader (Tecan GENios, Chapel Hill, NC) to read OD_{600} over 24 h as a proxy for cell growth. Relative growth inhibition was calculated by the average rate after normalizing the OD_{600} values in drug wells against the DMSO control wells on each assay plate.

Statistics. All data are expressed as means \pm standard deviations. No samples or animals were excluded from the analysis. For animal studies, group sizes were chosen when sufficient to reach a statistical power of at least 80% (http://www.statisticalsolutions.net/pss_calc.php). Mice were randomly assigned to treatment groups. Statistical analysis for survival studies was performed using Student-Newman-Keuls *t* test for multiple comparisons using INSTAT or by Kruskal-Wallis test. Statistical analysis for tissue burden and for trophic form and ascus counts was performed

using analysis of variance (ANOVA). Additional statistics were performed using unpaired *t* tests (comparison of two groups) or one-way ANOVA (comparison of three or more groups). Data met the assumption of a normal distribution as determined by statistical software, and variance was similar between groups that were statistically compared. Statistical tests were carried out using GraphPad Prism (La Jolla, CA) v. 400 software for Mac. Replicates used were biological replicates. Results were considered significant at $P \leq 0.05$.

Study approval. The mouse experiments were performed in full compliance with a protocol approved by Stony Brook University (study 341888-7; IACUC no. 2012-1967) and the University of Cincinnati Institutional Animal Care and Use Committee (ACORP no. 14-01-14-01), and in compliance with the 1966 Animal Welfare Act. The experiments were carried out in facilities accredited by the Association for Assessment and Accreditation of Laboratory Animal Care.

SUPPLEMENTAL MATERIAL

Supplemental material for this article may be found at <http://mbio.asm.org/lookup/suppl/doi:10.1128/mBio.00647-15/-/DCSupplemental>.

Table S1, PDF file, 0.05 MB.
Table S2, PDF file, 0.7 MB.
Table S3, PDF file, 0.1 MB.
Figure S1, PDF file, 0.5 MB.
Figure S2, PDF file, 0.7 MB.
Figure S3, PDF file, 0.6 MB.
Figure S4, PDF file, 0.5 MB.
Figure S5, PDF file, 0.8 MB.

ACKNOWLEDGMENTS

We thank Rao Movva for help with the HIP-HOP experiments. We thank the staff at the Transmission Electron Microscopy Facility in the Central Microscopy Imaging Center (C-MIC) at Stony Brook University, Stony Brook, NY, for their contributions to TEM preparation and data collection.

This work was supported by NIH-NIAID grants AI100631, AI56168, AI71142, and AI87541 to M.D.P. This work was also supported by NIH-NIAID Task Order A03: Expanded Screen for activity compound BHBM (to M.D.P.) and by NIH-NIAID HHSN272201000029I/HHSN27200002/A51 *Pneumocystis murina* Small Animal Model Utilization for Therapeutic Evaluation (to M.C.). This work was also supported by PhRMA Foundation Informatics Starter Grant to P.F., NIH-NHGRI grant HG004840 to X.P., and NIH-NIAID grant AI47837 to J.B.K. Leonardo Nimrichter and Marcio L. Rodrigues are supported by grants from Conselho Nacional de Desenvolvimento Tecnológico (CNPq, Brazil), CAPES, and Fundação Carlos Chagas Filho de Amparo à Pesquisa do Estado do Rio de Janeiro (FAPERJ, Brazil). Chiara Luberto is supported by DOD grant PRMRP Discovery award PR121476. Maurizio Del Poeta is a Burroughs Wellcome Investigator in the Pathogenesis of Infectious Diseases.

The funders have no role in the study design, data collection, and analysis, decision to publish, or preparation of the manuscript.

REFERENCES

1. Brown GD, Denning DW, Gow NA, Levitz SM, Netea MG, White TC. 2012. Hidden killers: human fungal infections. *Sci Transl Med* 4:165rv13. <http://dx.doi.org/10.1126/scitranslmed.3004404>.
2. Tuite NL, Lacey K. 2013. Overview of invasive fungal infections. *Methods Mol Biol* 968:1–23. http://dx.doi.org/10.1007/978-1-62703-257-5_1.
3. Morris AM. 2014. Review: voriconazole for prevention or treatment of invasive fungal infections in cancer with neutropenia. *Ann Intern Med* 161:JC8. <http://dx.doi.org/10.7326/0003-4819-161-2-201407150-02008>.
4. Lepak AJ, Andes DR. 2015. Antifungal pharmacokinetics and pharmacodynamics. *Cold Spring Harb Perspect Med* 5:a019653. <http://dx.doi.org/10.1101/cshperspect.a019653>.
5. Rittershaus PC, Kechichian TB, Allegood JC, Merrill AH, Jr, Hennig M, Luberto C, Del Poeta M. 2006. Glucosylceramide synthase is an essential regulator of pathogenicity of *Cryptococcus neoformans*. *J Clin Invest* 116:1651–1659. <http://dx.doi.org/10.1172/JCI27890>.

6. Singh A, Wang H, Silva LC, Na C, Prieto M, Futerman AH, Luberto C, Del Poeta M. 2012. Methylation of glycosylated sphingolipid modulates membrane lipid topography and pathogenicity of *Cryptococcus neoformans*. *Cell Microbiol* 14:500–516. <http://dx.doi.org/10.1111/j.1462-5822.2011.01735.x>.
7. Oura T, Kajiwara S. 2010. *Candida albicans* sphingolipid C9-methyltransferase is involved in hyphal elongation. *Microbiology* 156:1234–1243. <http://dx.doi.org/10.1099/mic.0.033985-0>.
8. Noble SM, French S, Kohn LA, Chen V, Johnson AD. 2010. Systematic screens of a *Candida albicans* homozygous deletion library decouple morphogenetic switching and pathogenicity. *Nat Genet* 42:590–598. <http://dx.doi.org/10.1038/ng.605>.
9. Lavery SB, Momany M, Lindsey R, Toledo MS, Shayman JA, Fuller M, Brooks K, Doong RL, Straus AH, Takahashi HK. 2002. Disruption of the glucosylceramide biosynthetic pathway in *Aspergillus nidulans* and *Aspergillus fumigatus* by inhibitors of UDP-Glc:ceramide glucosyltransferase strongly affects spore germination, cell cycle, and hyphal growth. *FEBS Lett* 525:59–64. [http://dx.doi.org/10.1016/S0014-5793\(02\)03067-3](http://dx.doi.org/10.1016/S0014-5793(02)03067-3).
10. Thevissen K, de Mello Tavares P, Xu D, Blankenship J, Vandenbosch D, Idkowiak-Baldys J, Govaert G, Bink A, Rozental S, de Groot PW, Davis TR, Kumamoto CA, Vargas G, Nimrichter L, Coenye T, Mitchell A, Roemer T, Hannun YA, Cammue BP. 2012. The plant defensin RsAFP2 induces cell wall stress, septin mislocalization and accumulation of ceramides in *Candida albicans*. *Mol Microbiol* 84:166–180. <http://dx.doi.org/10.1111/j.1365-2958.2012.08017.x>.
11. Rhome R, Singh A, Kechichian T, Drago M, Morace G, Luberto C, Del Poeta M. 2011. Surface localization of glucosylceramide during *Cryptococcus neoformans* infection allows targeting as a potential antifungal. *PLoS One* 6:e15572. <http://dx.doi.org/10.1371/journal.pone.0015572>.
12. Saito K, Takakuwa N, Ohnishi M, Oda Y. 2006. Presence of glucosylceramide in yeast and its relation to alkali tolerance of yeast. *Appl Microbiol Biotechnol* 71:515–521. <http://dx.doi.org/10.1007/s00253-005-0187-3>.
13. Rodrigues ML, Shi L, Barreto-Berger E, Nimrichter L, Farias SE, Rodrigues EG, Travassos LR, Nosanchuk JD. 2007. Monoclonal antibody to fungal glucosylceramide protects mice against lethal *Cryptococcus neoformans* infection. *Clin Vaccine Immunol* 14:1372–1376. <http://dx.doi.org/10.1128/CDVI.00202-07>.
14. Rittershaus PC, Kechichian TB, Allegood JC, Merrill AH, Hennig M, Luberto C, Del Poeta M. 2006. Glucosylceramide synthase is an essential regulator of pathogenicity of *Cryptococcus neoformans*. *J Clin Invest* 116:1651–1659. <http://dx.doi.org/10.1172/JCI27890>.
15. Oliveira DL, Nimrichter L, Miranda K, Frases S, Faull KF, Casadevall A, Rodrigues ML. 2009. *Cryptococcus neoformans* cryoultramicrotomy and vesicle fractionation reveals an intimate association between membrane lipids and glucuronoxylomannan. *Fungal Genet Biol* 46:956–963. <http://dx.doi.org/10.1016/j.fgb.2009.09.001>.
16. Rizzo J, Oliveira DL, Joffe LS, Hu G, Gazos-Lopes F, Fonseca FL, Almeida IC, Frases S, Kronstad JW, Rodrigues ML. 2014. Role of the Apt1 protein in polysaccharide secretion by *Cryptococcus neoformans*. *Eukaryot Cell* 13:715–726. <http://dx.doi.org/10.1128/EC.00273-13>.
17. Lo HJ, Köhler JR, DiDomenico B, Loebenberg D, Cacciapuoti A, Fink GR. 1997. Nonfilamentous *C. albicans* mutants are avirulent. *Cell* 90:939–949. [http://dx.doi.org/10.1016/S0092-8674\(00\)80358-X](http://dx.doi.org/10.1016/S0092-8674(00)80358-X).
18. Huang Z, Chen K, Xu T, Zhang J, Li Y, Li W, Agarwal AK, Clark AM, Phillips JD, Pan X. 2011. Sampangine inhibits heme biosynthesis in both yeast and human. *Eukaryot Cell* 10:1536–1544. <http://dx.doi.org/10.1128/EC.05170-11>.
19. Funato K, Riezman H. 2001. Vesicular and nonvesicular transport of ceramide from ER to the Golgi apparatus in yeast. *J Cell Biol* 155:949–959. <http://dx.doi.org/10.1083/jcb.200105033>.
20. Kajiwara K, Ikeda A, Aguilera-Romero A, Castillon GA, Kagiwada S, Hanada K, Riezman H, Muñoz M, Funato K. 2014. Osh proteins regulate COPII-mediated vesicular transport of ceramide from the endoplasmic reticulum in budding yeast. *J Cell Sci* 127:376–387. <http://dx.doi.org/10.1242/jcs.132001>.
21. Reggiori F, Conzelmann A. 1998. Biosynthesis of inositol phosphoceramides and remodeling of glycosylphosphatidylinositol anchors in *Saccharomyces cerevisiae* are mediated by different enzymes. *J Biol Chem* 273:30550–30559. <http://dx.doi.org/10.1074/jbc.273.46.30550>.
22. Rodrigues ML, Travassos LR, Miranda KR, Franzen AJ, Rozental S, de Souza W, Alviano CS, Barreto-Berger E. 2000. Human antibodies against a purified glucosylceramide from *Cryptococcus neoformans* inhibit cell budding and fungal growth. *Infect Immun* 68:7049–7060. <http://dx.doi.org/10.1128/IAI.68.12.7049-7060.2000>.
23. Suzuki Y, St Onge RP, Mani R, King OD, Heilbut A, Labunsky VM, Chen W, Pham L, Zhang LV, Tong AH, Nislow C, Giaever G, Gladyshev VN, Vidal M, Schow P, Lehár J, Roth FP. 2011. Knocking out multigene redundancies via cycles of sexual assortment and fluorescence selection. *Nat Methods* 8:159–164. <http://dx.doi.org/10.1038/nmeth.1550>.
24. Knaus M, Pelli-Gulli MP, van Drogen F, Springer S, Jaquenoud M, Peter M. 2007. Phosphorylation of Bem2p and Bem3p may contribute to local activation of Cdc42p at bud emergence. *EMBO J* 26:4501–4513. <http://dx.doi.org/10.1038/sj.emboj.7601873>.
25. Elia L, Marsh L. 1998. A role for a protease in morphogenic responses during yeast cell fusion. *J Cell Biol* 142:1473–1485. <http://dx.doi.org/10.1083/jcb.142.6.1473>.
26. Merchan S, Pedelini L, Hueso G, Calzada A, Serrano R, Yenush L. 2011. Genetic alterations leading to increases in internal potassium concentrations are detrimental for DNA integrity in *Saccharomyces cerevisiae*. *Genes Cells* 16:152–165. <http://dx.doi.org/10.1111/j.1365-2443.2010.01472.x>.
27. Tong Z, Gao XD, Howell AS, Bose I, Lew DJ, Bi E. 2007. Adjacent positioning of cellular structures enabled by a Cdc42 GTPase-activating protein-mediated zone of inhibition. *J Cell Biol* 179:1375–1384. <http://dx.doi.org/10.1083/jcb.200705160>.
28. Finley D, Ulrich HD, Sommer T, Kaiser P. 2012. The ubiquitin-proteasome system of *Saccharomyces cerevisiae*. *Genetics* 192:319–360. <http://dx.doi.org/10.1534/genetics.112.140467>.
29. Mulholland J, Wesp A, Riezman H, Botstein D. 1997. Yeast actin cytoskeleton mutants accumulate a new class of Golgi-derived secretory vesicle. *Mol Biol Cell* 8:1481–1499. <http://dx.doi.org/10.1091/mbc.8.8.1481>.
30. Narang R, Narasimhan B, Sharma S. 2012. A review on biological activities and chemical synthesis of hydrazide derivatives. *Curr Med Chem* 19:569–612. <http://dx.doi.org/10.2174/092986712798918789>.
31. Rollas S, Küçükgüzel SG. 2007. Biological activities of hydrazone derivatives. *Molecules* 12:1910–1939. <http://dx.doi.org/10.3390/12081910>.
32. Verma G, Marella A, Shaquiquzzaman M, Akhtar M, Ali MR, Alam MM. 2014. A review exploring biological activities of hydrazones. *J Pharm Bioallied Sci* 6:69–80. <http://dx.doi.org/10.4103/0975-7406.129170>.
33. Altıntop MD, Özdemir A, Turan-Zitouni G, İlgin S, Atlı Ö, İşcan G, Kaplancıklı ZA. 2012. Synthesis and biological evaluation of some hydrazone derivatives as new anticandidal and anticancer agents. *Eur J Med Chem* 58:299–307. <http://dx.doi.org/10.1016/j.ejmech.2012.10.011>.
34. Kumar P, Narasimhan B. 2013. Hydrazides/hydrazones as antimicrobial and anticancer agents in the new millennium. *Mini Rev Med Chem* 13:971–987. <http://dx.doi.org/10.2174/1389557511313070003>.
35. Maillard LT, Bertout S, Quinonero O, Akalin G, Turan-Zitouni G, Fulcrand P, Demirci F, Martinez J, Masurier N. 2013. Synthesis and anti-*Candida* activity of novel 2-hydrazino-1,3-thiazole derivatives. *Bioorg Med Chem Lett* 23:1803–1807. <http://dx.doi.org/10.1016/j.bmcl.2013.01.039>.
36. Secci D, Bizzarri B, Bolasco A, Carradori S, D’Ascenzio M, Rivarera D, Mari E, Polletta L, Zicari A. 2012. Synthesis, anti-*Candida* activity, and cytotoxicity of new (4-(4-iodophenyl)thiazol-2-yl)hydrazine derivatives. *Eur J Med Chem* 53:246–253. <http://dx.doi.org/10.1016/j.ejmech.2012.04.006>.
37. Coelho C, Bocca AL, Casadevall A. 2014. The intracellular life of *Cryptococcus neoformans*. *Annu Rev Pathol* 9:219–238. <http://dx.doi.org/10.1146/annurev-pathol-012513-104653>.
38. Kechichian TB, Shea J, Del Poeta M. 2007. Depletion of alveolar macrophages decreases the dissemination of a glucosylceramide-deficient mutant of *Cryptococcus neoformans* in immunodeficient mice. *Infect Immun* 75:4792–4798. <http://dx.doi.org/10.1128/IAI.00587-07>.
39. Gallis HA, Drew RH, Pickard WW. 1990. Amphotericin B: 30 years of clinical experience. *Rev Infect Dis* 12:308–329. <http://dx.doi.org/10.1093/clinids/12.2.308>.
40. Sawaya BP, Briggs JP, Schnermann J. 1995. Amphotericin B nephrotoxicity: the adverse consequences of altered membrane properties. *J Am Soc Nephrol* 6:154–164.
41. Lobo ML, Esteves F, de Sousa B, Cardoso F, Cushion MT, Antunes F, Matos O. 2013. Therapeutic potential of caspofungin combined with trimethoprim-sulfamethoxazole for pneumocystis pneumonia: a pilot study in mice. *PLoS One* 8:e70619. <http://dx.doi.org/10.1371/journal.pone.0070619>.

42. Miyazaki T, Miyazaki Y, Izumikawa K, Kakeya H, Miyakoshi S, Bennett JE, Kohno S. 2006. Fluconazole treatment is effective against a *Candida albicans* *erg3/erg3* mutant in vivo despite in vitro resistance. *Antimicrob Agents Chemother* 50:580–586. <http://dx.doi.org/10.1128/AAC.50.2.580-586.2006>.
43. Giaever G, Nislow C. 2014. The yeast deletion collection: a decade of functional genomics. *Genetics* 197:451–465. <http://dx.doi.org/10.1534/genetics.114.161620>.
44. Cowles CR, Odorizzi G, Payne GS, Emr SD. 1997. The AP-3 adaptor complex is essential for cargo-selective transport to the yeast vacuole. *Cell* 91:109–118. [http://dx.doi.org/10.1016/S0092-8674\(01\)80013-1](http://dx.doi.org/10.1016/S0092-8674(01)80013-1).
45. Robinson MS. 2004. Adaptable adaptors for coated vesicles. *Trends Cell Biol* 14:167–174. <http://dx.doi.org/10.1016/j.tcb.2004.02.002>.
46. Angers CG, Merz AJ. 2009. HOPS interacts with Apl5 at the vacuole membrane and is required for consumption of AP-3 transport vesicles. *Mol Biol Cell* 20:4563–4574. <http://dx.doi.org/10.1091/mbc.E09-04-0272>.
47. Schuldiner M, Collins SR, Thompson NJ, Denic V, Bhamidipati A, Punna T, Ihmels J, Andrews B, Boone C, Greenblatt JF, Weissman JS, Krogan NJ. 2005. Exploration of the function and organization of the yeast early secretory pathway through an epistatic miniarray profile. *Cell* 123:507–519. <http://dx.doi.org/10.1016/j.cell.2005.08.031>.
48. Ptacek J, Devgan G, Michaud G, Zhu H, Zhu X, Fasolo J, Guo H, Jona G, Breitkreutz A, Sopko R, McCartney RR, Schmidt MC, Rachidi N, Lee SJ, Mah AS, Meng L, Stark MJ, Stern DF, De Virgilio C, Tyers M, Andrews B, Gerstein M, Schweitzer B, Predki PF, Snyder M. 2005. Global analysis of protein phosphorylation in yeast. *Nature* 438:679–684. <http://dx.doi.org/10.1038/nature04187>.
49. Kolawa N, Sweredoski MJ, Graham RL, Oania R, Hess S, Deshaies RJ. 2013. Perturbations to the ubiquitin conjugate proteome in yeast Δubx mutants identify Ubx2 as a regulator of membrane lipid composition. *Mol Cell Proteomics* 12:2791–2803. <http://dx.doi.org/10.1074/mcp.M113.030163>.
50. Swaney DL, Beltrao P, Starita L, Guo A, Rush J, Fields S, Krogan NJ, Villén J. 2013. Global analysis of phosphorylation and ubiquitylation cross-talk in protein degradation. *Nat Methods* 10:676–682. <http://dx.doi.org/10.1038/nmeth.2519>.
51. Hicke L, Riezman H. 1996. Ubiquitination of a yeast plasma membrane receptor signals its ligand-stimulated endocytosis. *Cell* 84:277–287. [http://dx.doi.org/10.1016/S0092-8674\(00\)80982-4](http://dx.doi.org/10.1016/S0092-8674(00)80982-4).
52. Peng J, Schwartz D, Elias JE, Thoreen CC, Cheng D, Marsischky G, Roelofs J, Finley D, Gygi SP. 2003. A proteomics approach to understanding protein ubiquitination. *Nat Biotechnol* 21:921–926. <http://dx.doi.org/10.1038/nbt849>.
53. Mandala SM, Thornton RA, Frommer BR, Dreikorn S, Kurtz MB. 1997. Viridifungins, novel inhibitors of sphingolipid synthesis. *J Antibiot* 50: 339–343. <http://dx.doi.org/10.7164/antibiotics.50.339>.
54. Bligh EG, Dyer WJ. 1959. A rapid method for total lipid extraction and purification. *Can J Biochem Physiol* 37:911–917.
55. Clinical and Laboratory Standards Institute. 2008. Reference method for broth dilution antifungal susceptibility testing of yeasts; approved standard—third edition. CLSI document M27-A3. Clinical and Laboratory Standards Institute, Wayne, PA.
56. Cordero RJ, Pontes B, Frases S, Nakouzi AS, Nimrichter L, Rodrigues ML, Viana NB, Casadevall A. 2013. Antibody binding to *Cryptococcus neoformans* impairs budding by altering capsular mechanical properties. *J Immunol* 190:317–323. <http://dx.doi.org/10.4049/jimmunol.1202324>.
57. Heung LJ, Kaiser AE, Luberto C, Del Poeta M. 2005. The role and mechanism of diacylglycerol-protein kinase C1 signaling in melanogenesis by *Cryptococcus neoformans*. *J Biol Chem* 280:28547–28555. <http://dx.doi.org/10.1074/jbc.M503404200>.
58. Pierce SE, Davis RW, Nislow C, Giaever G. 2007. Genome-wide analysis of barcoded *Saccharomyces cerevisiae* gene-deletion mutants in pooled cultures. *Nat Protoc* 2:2958–2974. <http://dx.doi.org/10.1038/nprot.2007.427>.
59. Proctor M, Urbanus ML, Fung EL, Jaramillo DF, Davis RW, Nislow C, Giaever G. 2011. The automated cell: compound and environment screening system (ACCESS) for chemogenomic screening. *Methods Mol Biol* 759:239–269. http://dx.doi.org/10.1007/978-1-61779-173-4_15.
60. Hoffman CS, Winston F. 1987. A ten-minute DNA preparation from yeast efficiently releases autonomous plasmids for transformation of *Escherichia coli*. *Gene* 57:267–272. [http://dx.doi.org/10.1016/0378-1119\(87\)90131-4](http://dx.doi.org/10.1016/0378-1119(87)90131-4).
61. Li R, Yu C, Li Y, Lam T-W, Yiu S-M, Kristiansen K, Wang J. 2009. SOAP2: an improved ultrafast tool for short read alignment. *Bioinformatics* 25:1966–1967. <http://dx.doi.org/10.1093/bioinformatics/btp336>.
62. McKenna A, Hanna M, Banks E, Sivachenko A, Cibulskis K, Kernysky A, Garimella K, Altshuler D, Gabriel S, Daly M, DePristo MA. 2010. The Genome Analysis Toolkit: a MapReduce framework for analyzing next-generation DNA sequencing data. *Genome Res* 20:1297–1303. <http://dx.doi.org/10.1101/gr.107524.110>.
63. DePristo MA, Banks E, Poplin R, Garimella KV, Maguire JR, Hartl C, Philippakis AA, del Angel G, Rivas MA, Hanna M, McKenna A, Fennell TJ, Kernysky AM, Sivachenko AY, Cibulskis K, Gabriel SB, Altshuler D, Daly MJ. 2011. A framework for variation discovery and genotyping using next-generation DNA sequencing data. *Nat Genet* 43:491–498. <http://dx.doi.org/10.1038/ng.806>.